Summer 6-24-2014

New class of refractory ceramics for thermal barrier coatings

Wei Pan
School of Material Science and Engineering, Tsinghua University

New Class of Refractory Ceramics for Thermal Barrier Coatings

Wei Pan
School of Materials Science and Engineering
Tsinghua University, Beijing, China
2014/06/24

Low thermal conductivity oxides

Gas outlet and make gas film on the surface of ceramic

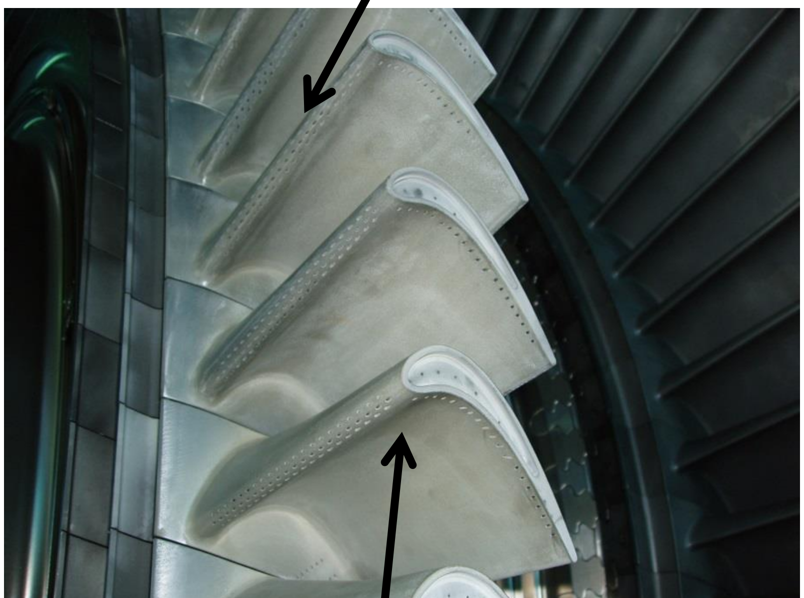

Ceramic coating on the surface of blade

No candidate materials take the position of YSZ owing to their comprehensive properties.

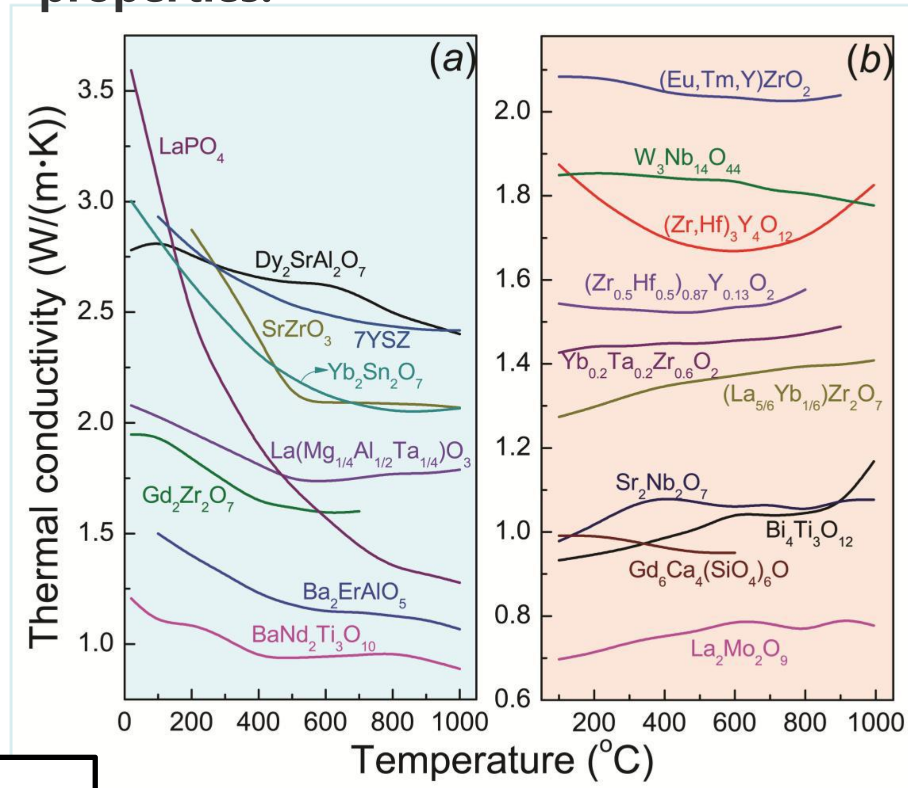

W Pan, Simon R. Phillpot, Chunlei Wan, Aleksandr Chernatynskiy, Zhixue Qu, MRS Bulletin, Vol. 37, Oct. 2012, p917

Principle for reducing the thermal conductivity

$$\kappa = \frac{1}{3} c_V \cdot v \cdot \lambda$$

$$\frac{1}{\lambda(\omega,T)} = \frac{1}{\lambda_u(\omega,T)} + \frac{1}{\lambda_p(\omega,T)} + \frac{1}{\lambda_b}$$

- ***Decrease the sound velocity***

  Elastic's modulus, molecular weight

- ***Decrease the phonon mean free path***

  Increasing the phonon scattering

Principle for reducing the thermal conductivity

- ***Introduce defects in the crystal***
  - Increasing the concentration of vacancy
  - Introduce substitutions
  - Increasing the structure distortion
- ***Increase the complexity***
  - Complex structure
  - Anisotropic structure

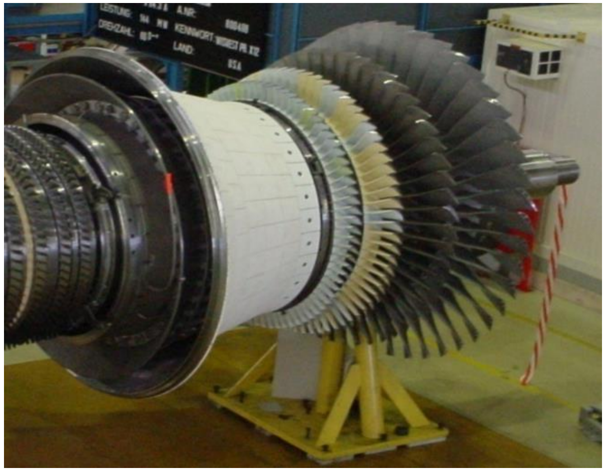

Main parameter of structure distortion for point defects

Phonon scattering coefficient by point defects

$$\Gamma_i = f_i\{(\Delta M_i / M)^2 + 2[(\Delta G_i / G) - 6.4\gamma(\Delta \delta_i / \delta)]^2\}$$

$\Delta M_i / M$ **Mass difference**

$\Delta G_i / G$ **Atomic interaction force difference**

$\Delta \delta_i / \delta$ **Size difference**

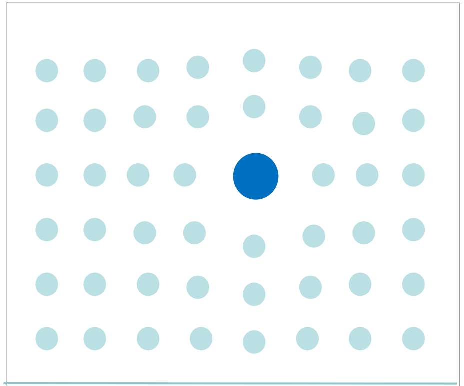

Lattice distortion

Anharmonic parameter *γ*

$$\gamma = 3\alpha_l K /(C_p \rho)$$

α_l: thermal expansion coefficient, K:bulk modulus, C_p: heat capacity, ρ:density

Temperature correction of elastic constants

$$E(T) = E_0 - 0.0645(T - T_0)$$

CL Wan, W Pan, et al, Phys. Rev. B 74,144109-1~9 (2006).

High oxygen vacancy concentration oxides

Oxygen vacancies in oxide ceramics

Perfect crystal

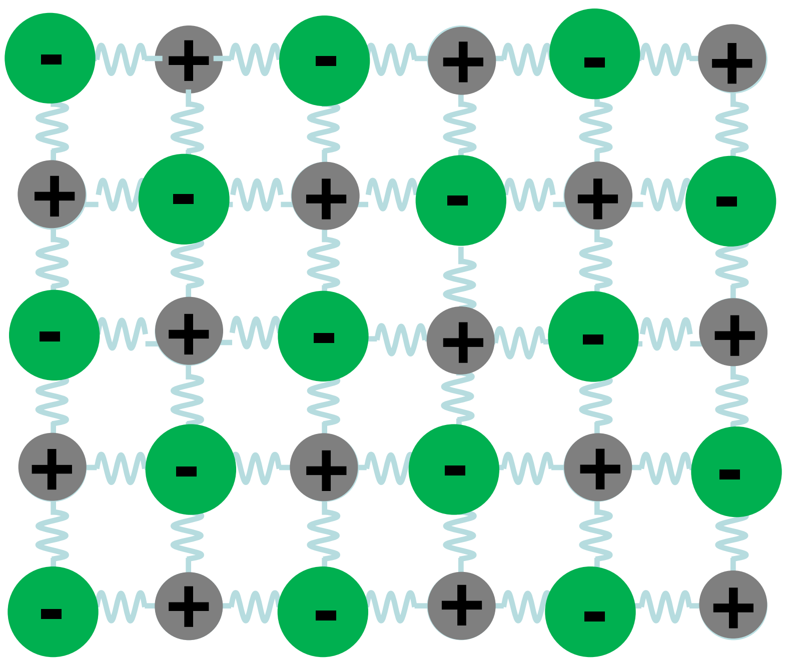

Defect crystal

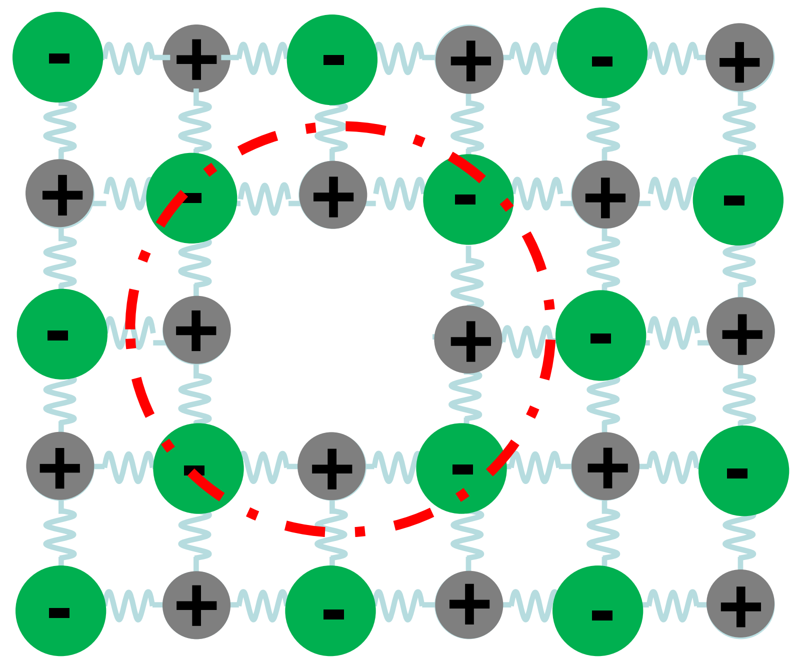

Highly anharmonic area with weak bonding

$$\Gamma_i = f_i\{(\Delta M_i / M)^2 + 2[(\Delta G_i / G) - 6.4\gamma(\Delta\delta_i / \delta)]^2\}$$

Phonon scattering coefficient is significant in the oxygen defect crystal!

Oxygen vacancy- a guide of low thermal conductive ceramics

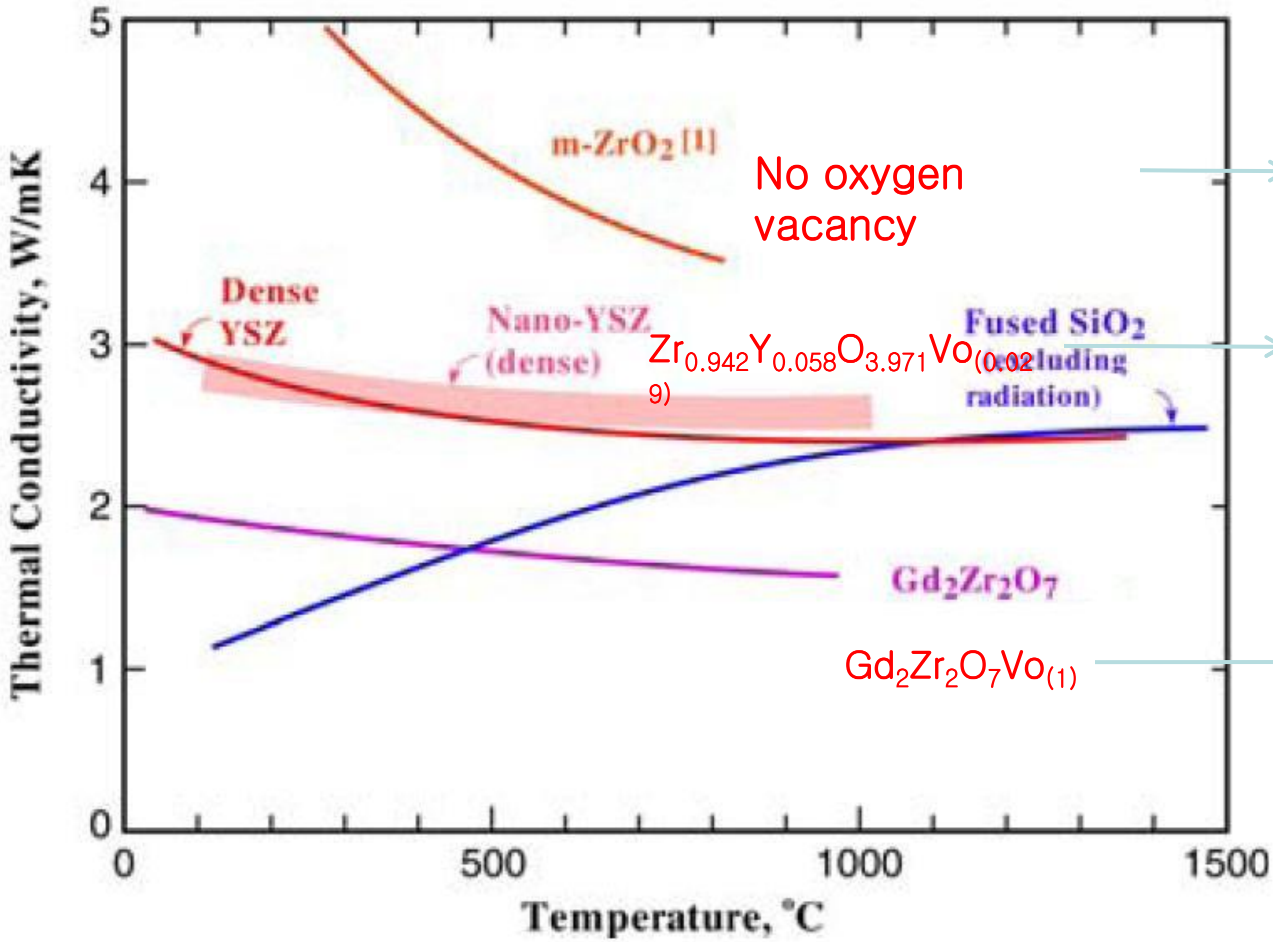

Vo/O=0

Vo/O=0.029/4

Vo/O=1/8

Thermal conductivity decreases with the increase of oxygen defect concentration!

Low thermal conductivity of Ba_2ReAlO_5 compounds

The oxygen vacancy concentration is 1/6!

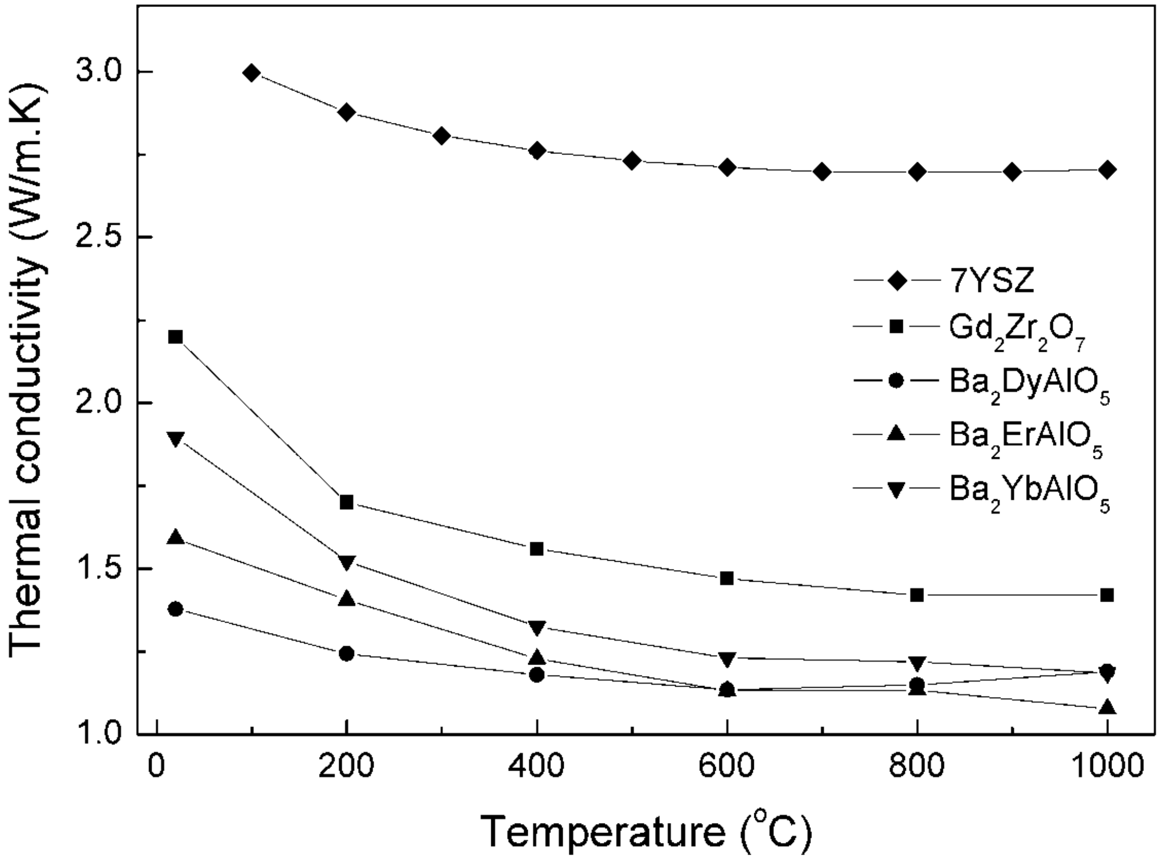

Wan CL, W Pan et al, Phys. Rev. Lett. 101, 085901 (2008).

Phonon mean free path of Ba_2ReAlO_5 compounds

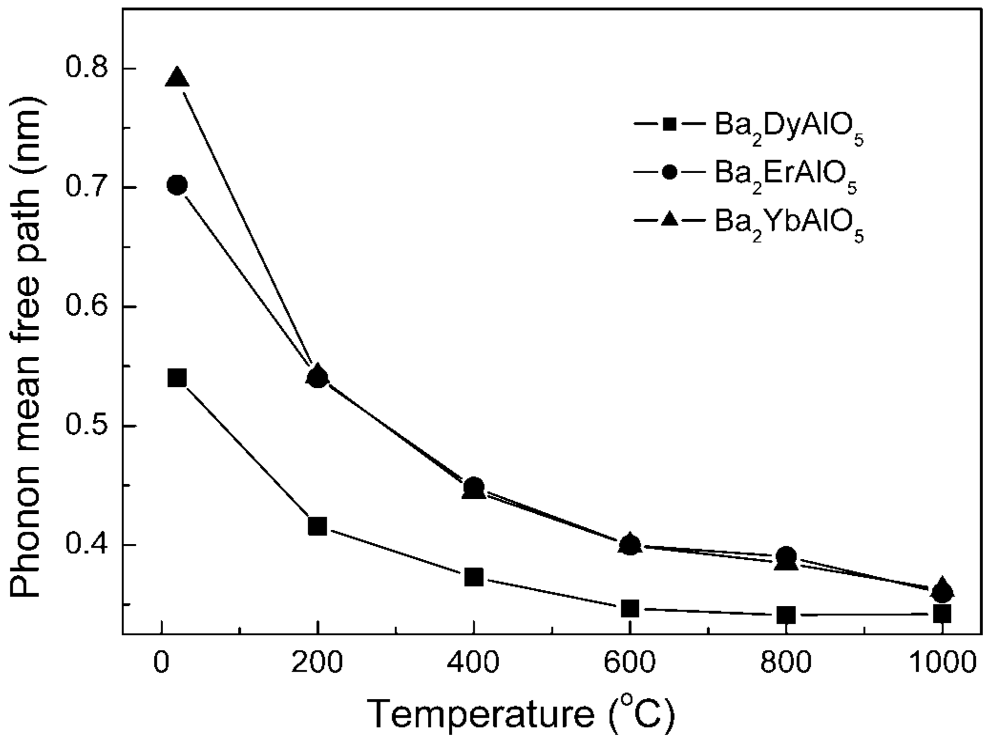

•Lattice constant of Ba_2DyAlO_5:
a=0.7239nm, b=0.7449nm, c=0.6035nm

•Interatomic distance of Ba_2ReAlO_5
Re=Dy, a=0.24nm; Re=Er, a=0.24nm;
Re=Yb, a=0.23nm

Wan CL, W Pan et al, Phys. Rev. Lett. 101, 085901 (2008).

Thermal expansion coefficients of Ba_2ReAlO_5 compounds

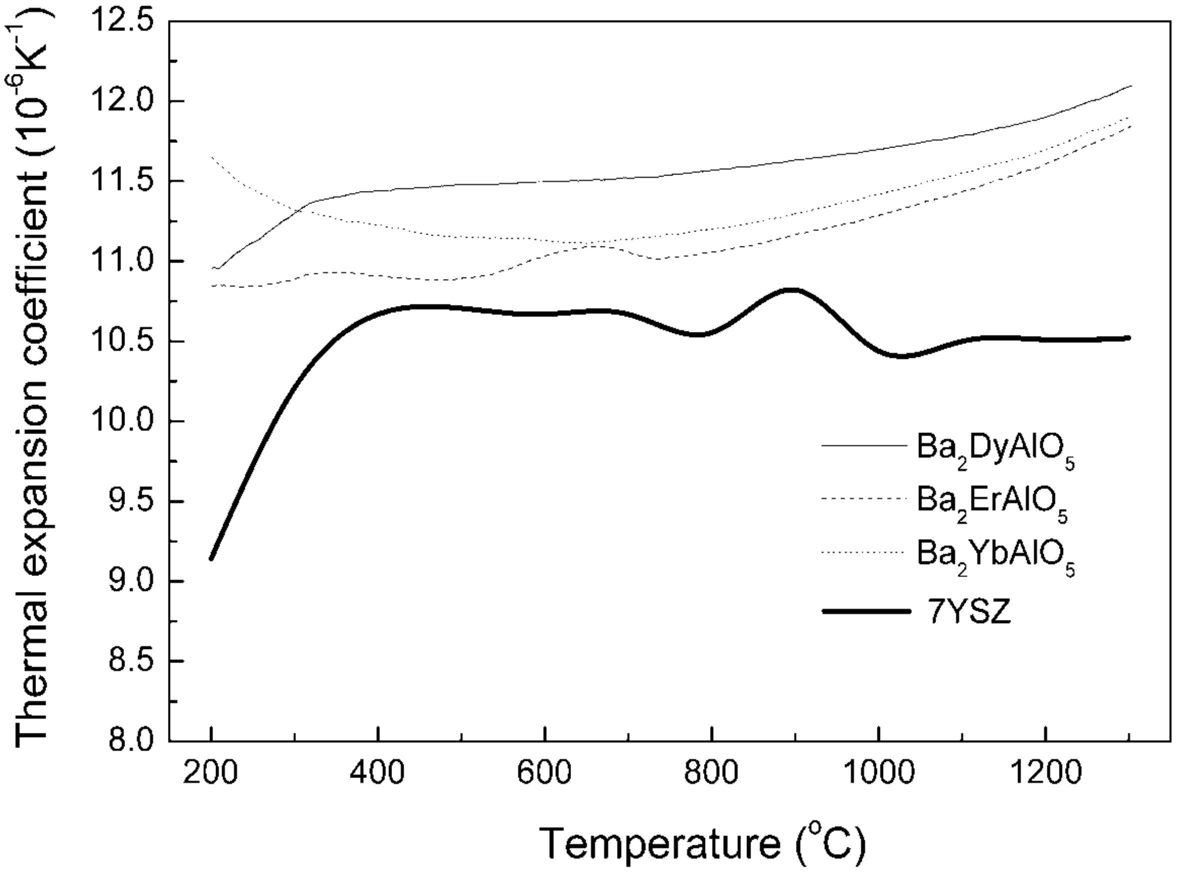

Wan CL, W Pan et al, Phys. Rev. Lett. 101, 085901 (2008).

Thermal conductivity of $Ba_6Ln_2Al_4O_{15}$

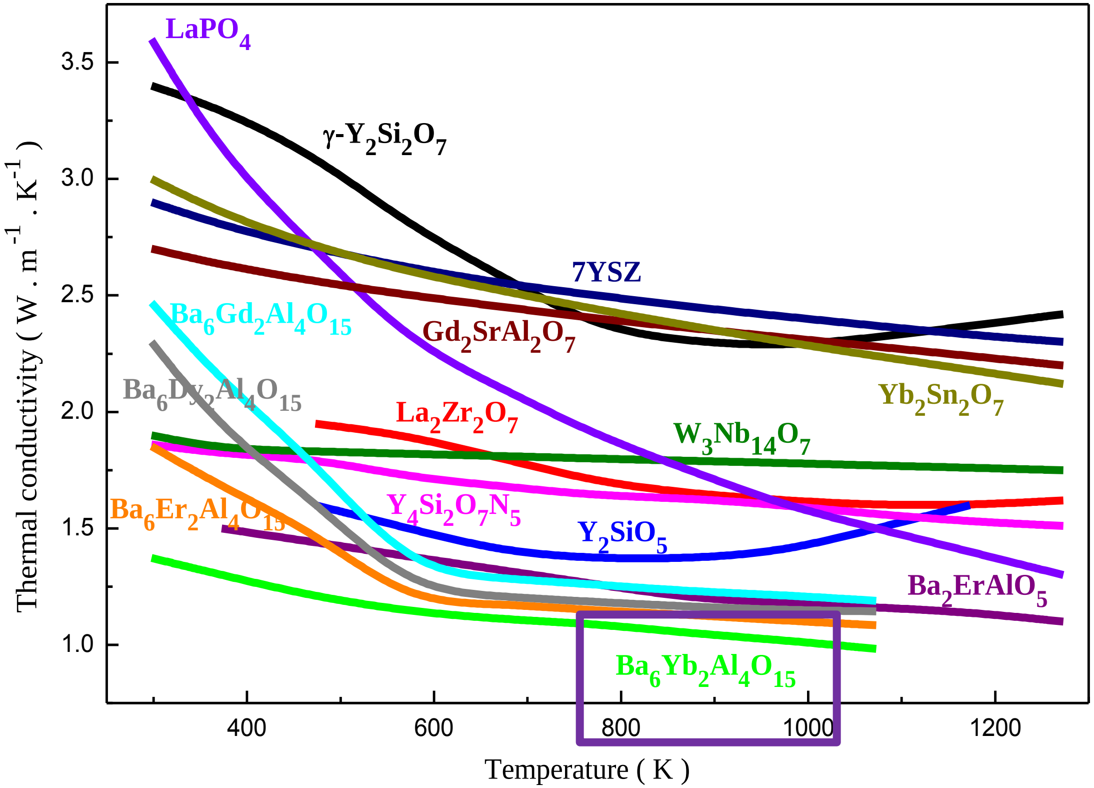

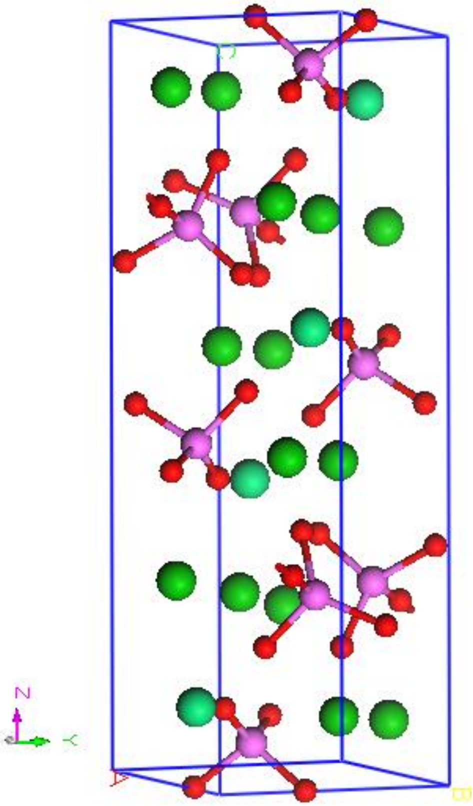

Vo/O=1/6

High thermal expansions of the $Ba_6Ln_2Al_4O_{15}$ compounds

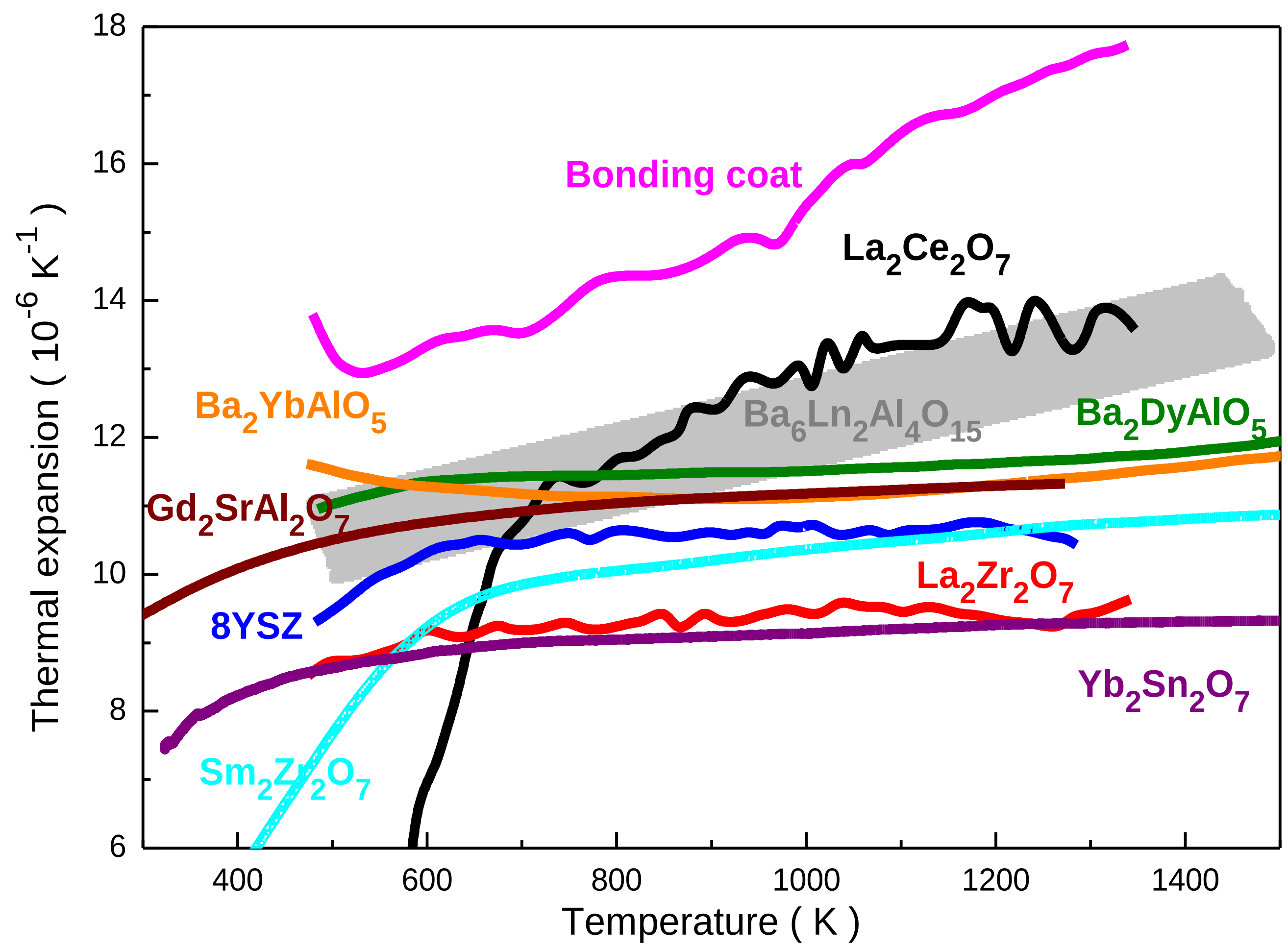

Effect of anion and cation defects on the thermal conductivity

$$Gd_{8+x}Ca_{2+y}(SiO_4)_6O_{2+3x/2+y}$$

Zhixue Qu, Taylor D. Sparks, Wei Pan, David R. Clarke, *Acta Mater.* 59 (2011) 3841–3850

Variations in composition from the stoichiometric composition according to the formula $Gd_{8+x}Ca_{2+y}(SiO_4)_6O_{2+3x/2+y}$.

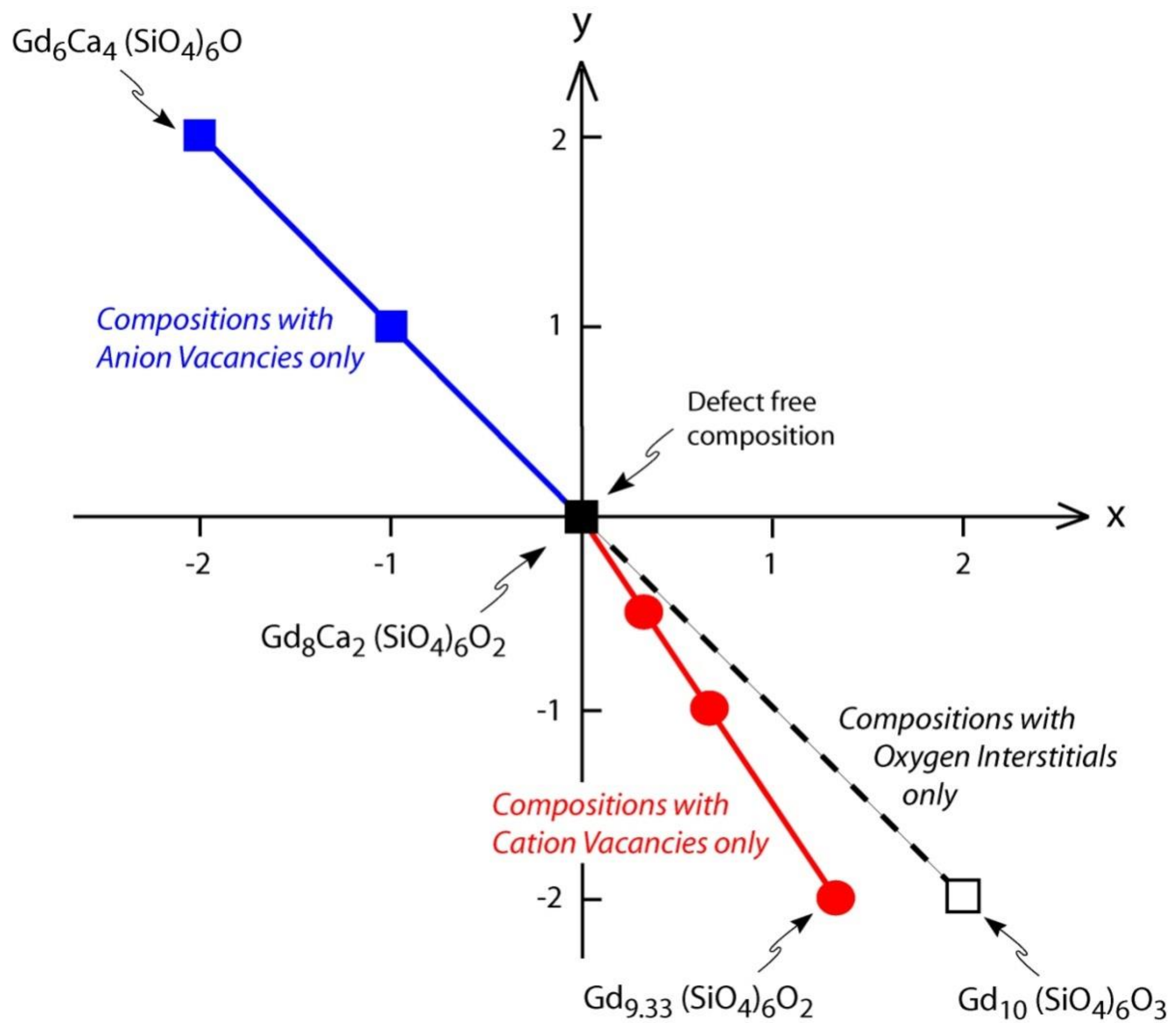

Zhixue Qu, Taylor D. Sparks, Wei Pan, David R. Clarke, *Acta Mater.* 59 (2011) 3841–3850

Thermal conductivity as a function of nominal defect concentration per unit cell.

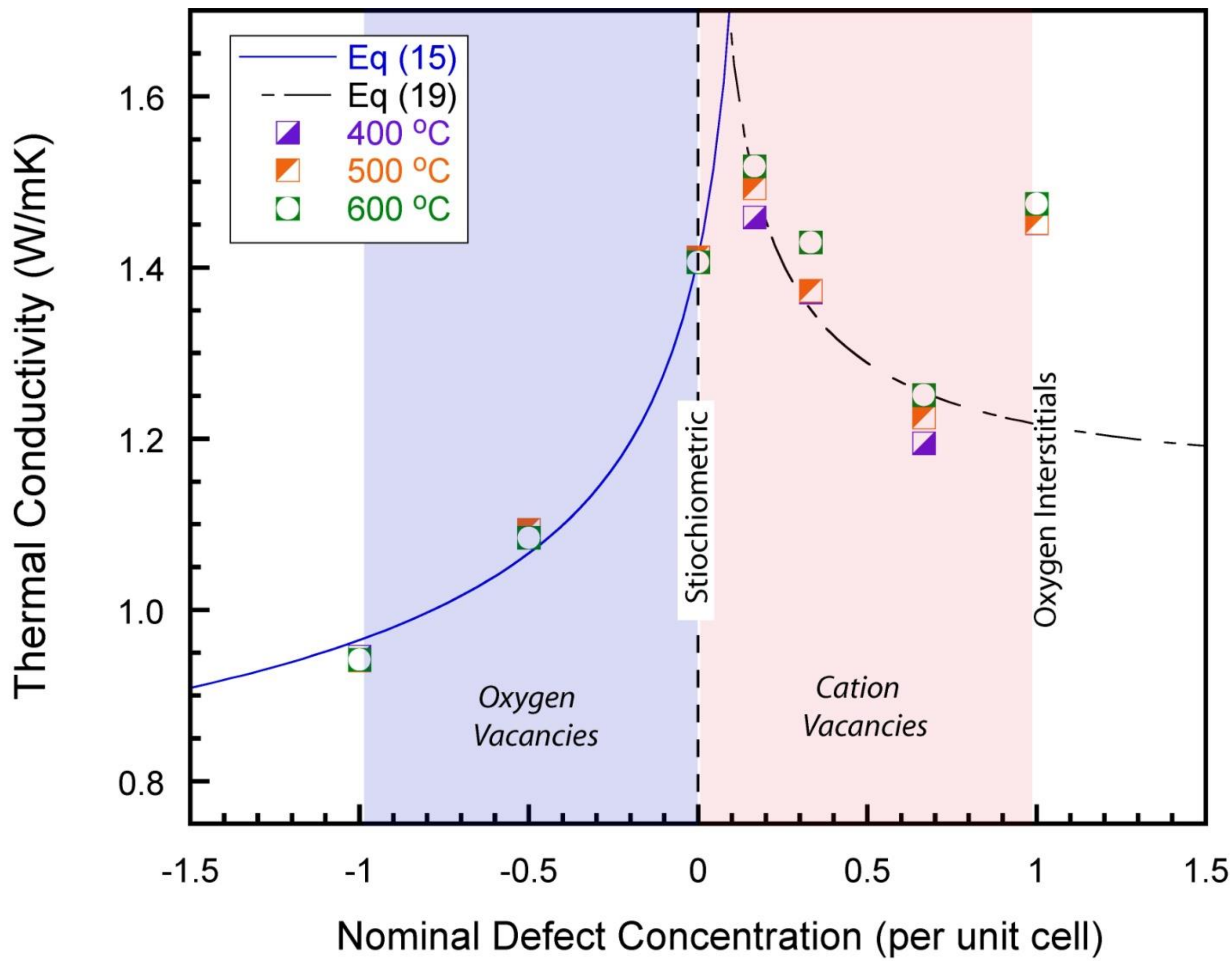

Zhixue Qu, Taylor D. Sparks, Wei Pan, David R. Clarke, *Acta Mater.* **59 (2011) 3841–3850**

Substitution of atoms, alloying in oxides

(pyrochlore and fluorite $A_2B_2O_7$ oxides)

Substitution defects in oxide ceramics

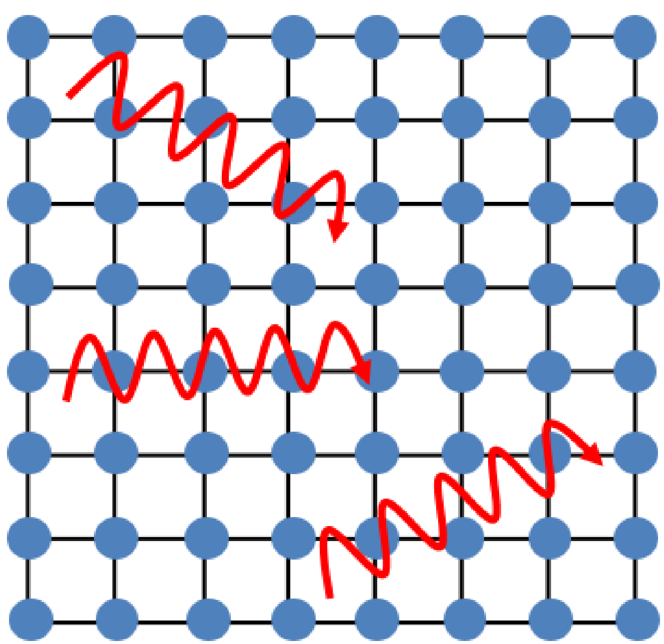

Perfect lattice

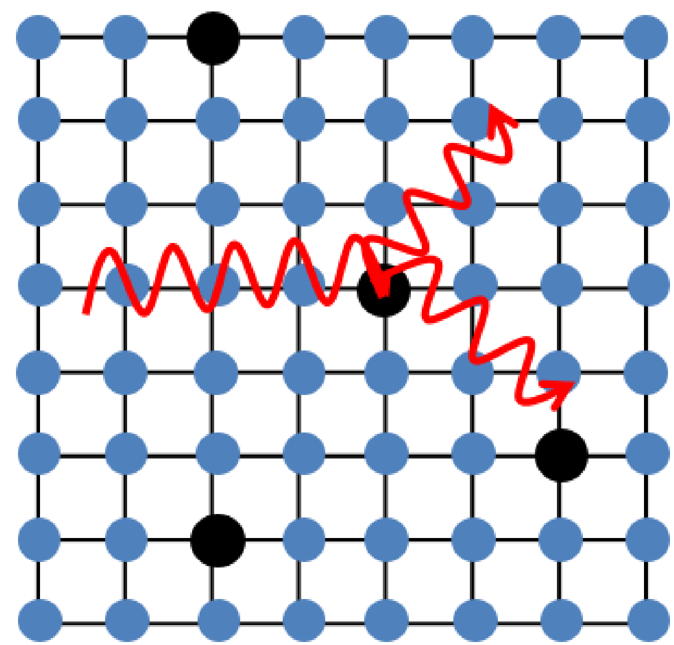

Defective lattice
Phonon scattering

$(La_{1-x}Gd_x)_2Zr_2O_7$ pyrochlores

Small difference of doping ion size at “A” site:

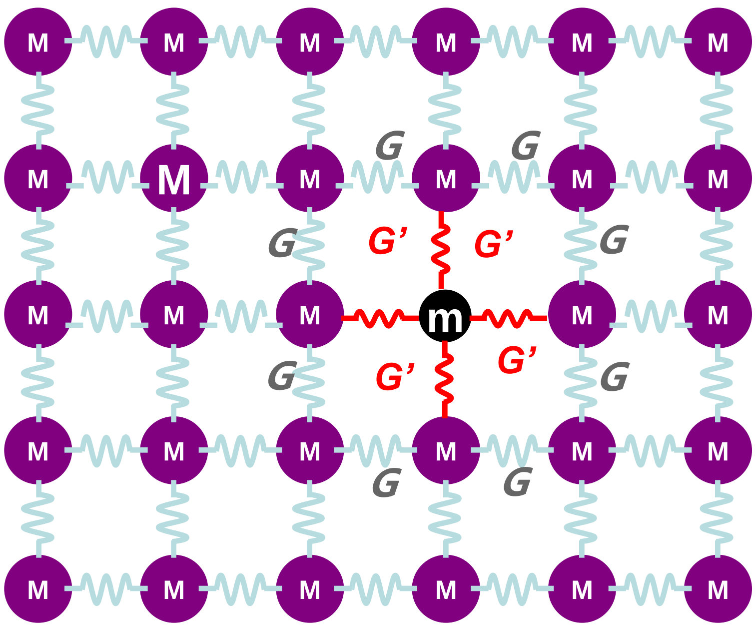

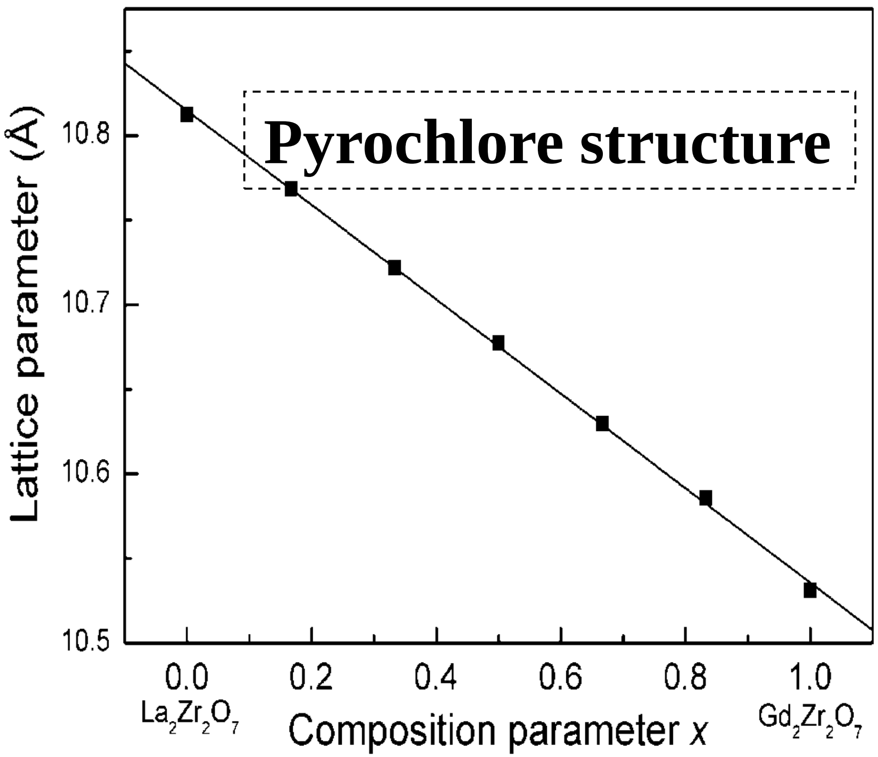

Lattice parameter

CL Wan, W Pan, et al, *Phys. Rev. B*, 74, 144109 (2006).

Thermal conductivities of $(La_{1-x}Gd_x)_2Zr_2O_7$

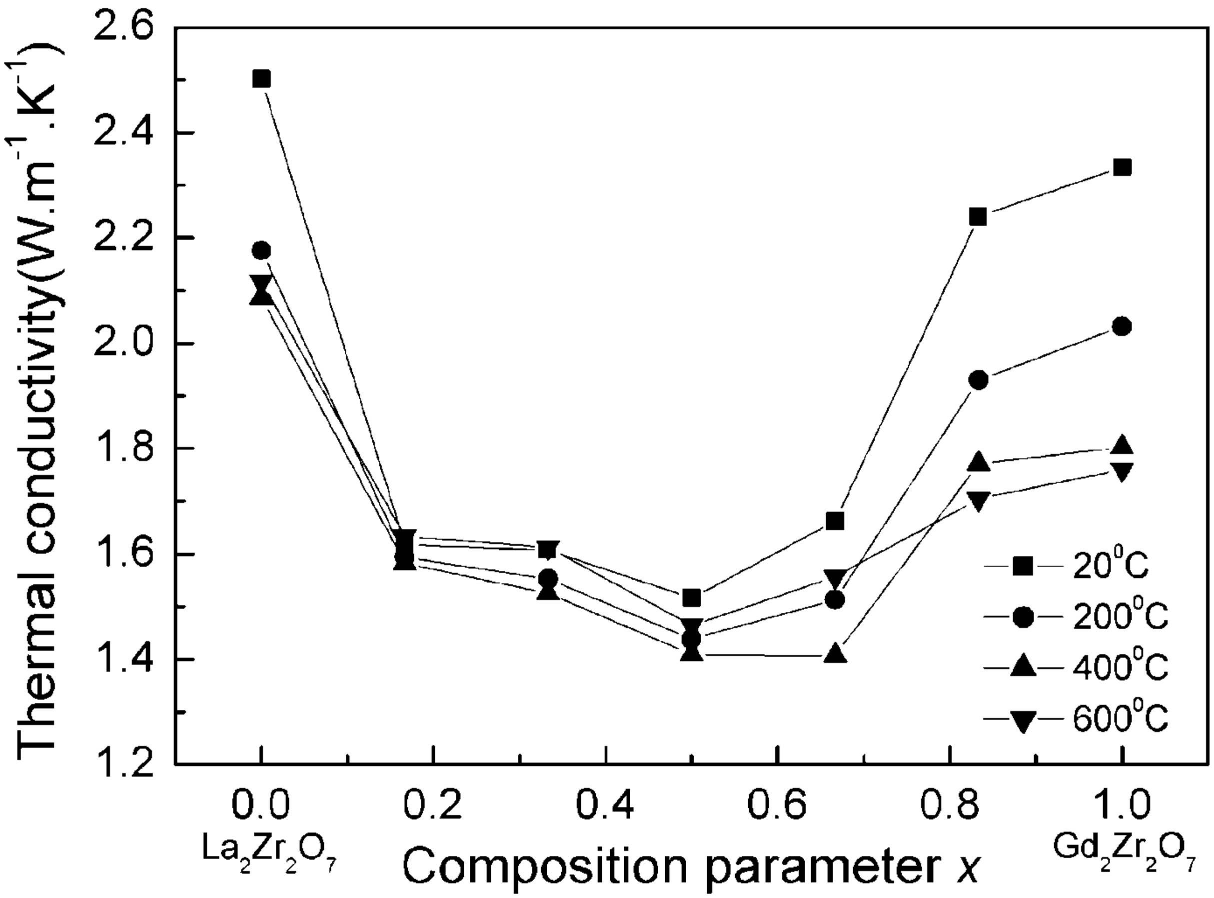

CL Wan, W Pan, et al, *Phys. Rev. B*, 74, 144109 (2006).

Lattice softening in $(La_{1-x}Gd_x)_2Zr_2O_7$

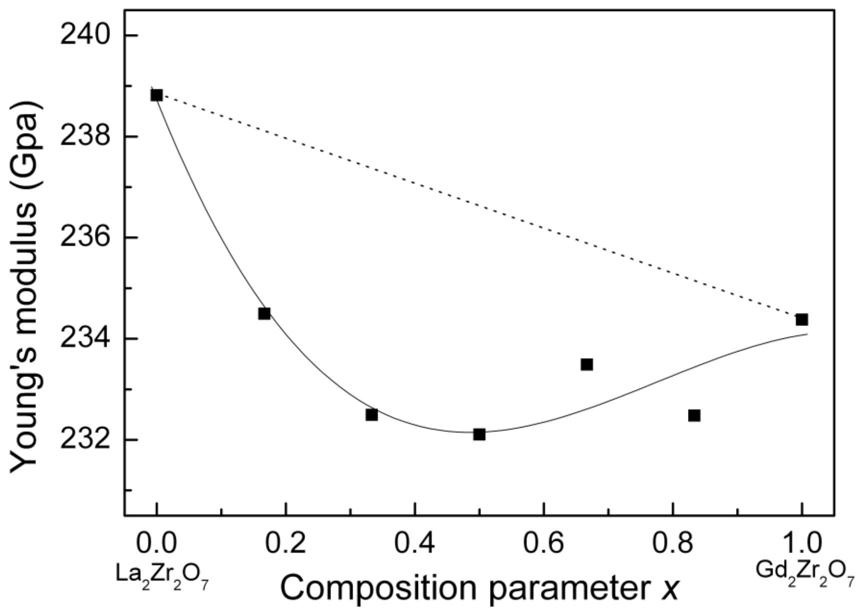

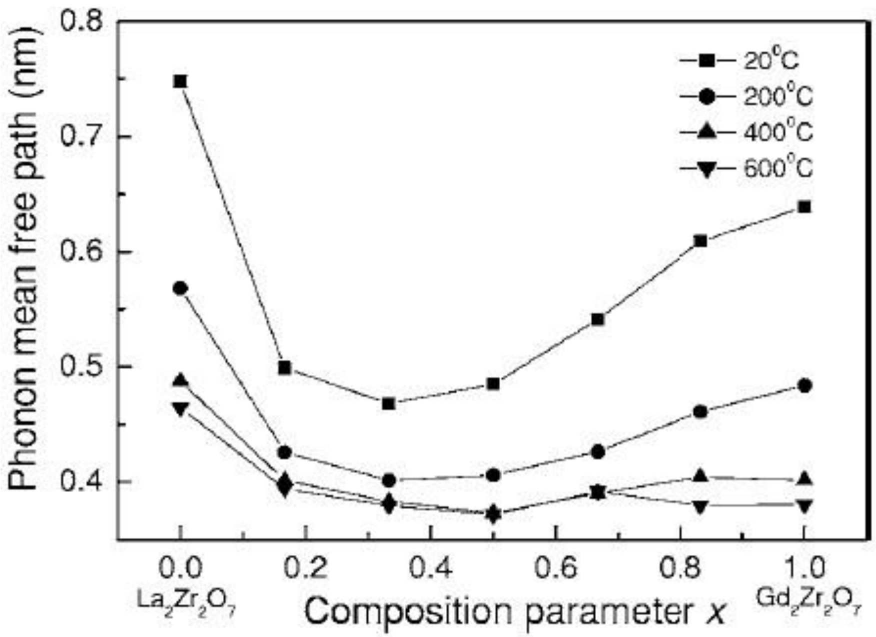

Young's modulus (Average sound velocity)

Phonon mean free path

CL Wan, W Pan, et al, *Phys. Rev. B*, 74, 144109 (2006).

$(La_{1-x}Yb_x)_2Zr_2O_7$ pyrochlores

Big difference of doping ion size at "A" site:

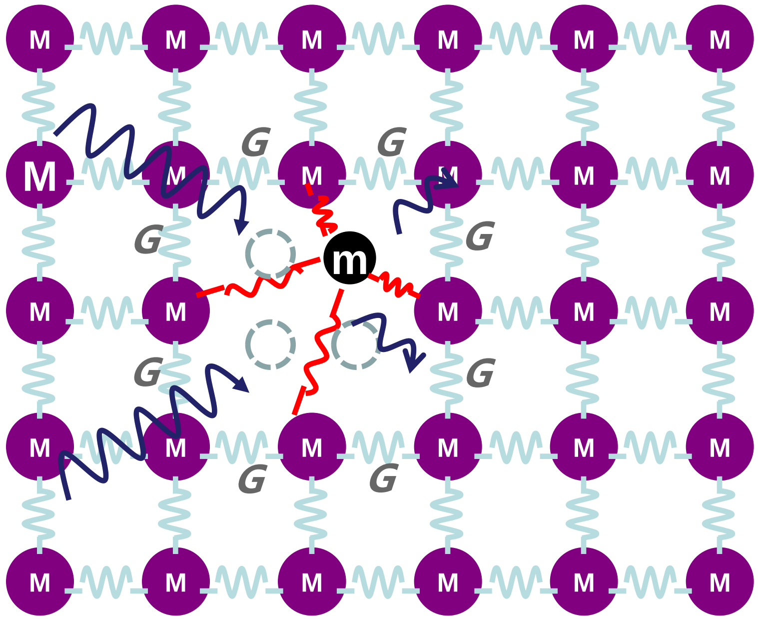

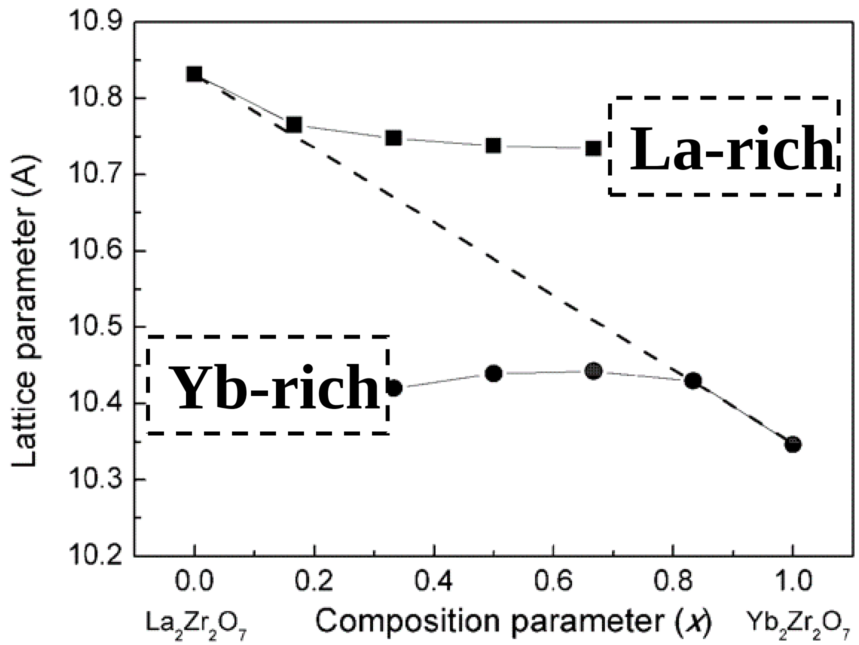

Double phase structure

Wan CL, W Pan et al. *Acta Mater.*, 58, 6166–6172, (2010).

Thermal conductivities of $(La_{1-x}Gd_x)_2Zr_2O_7$

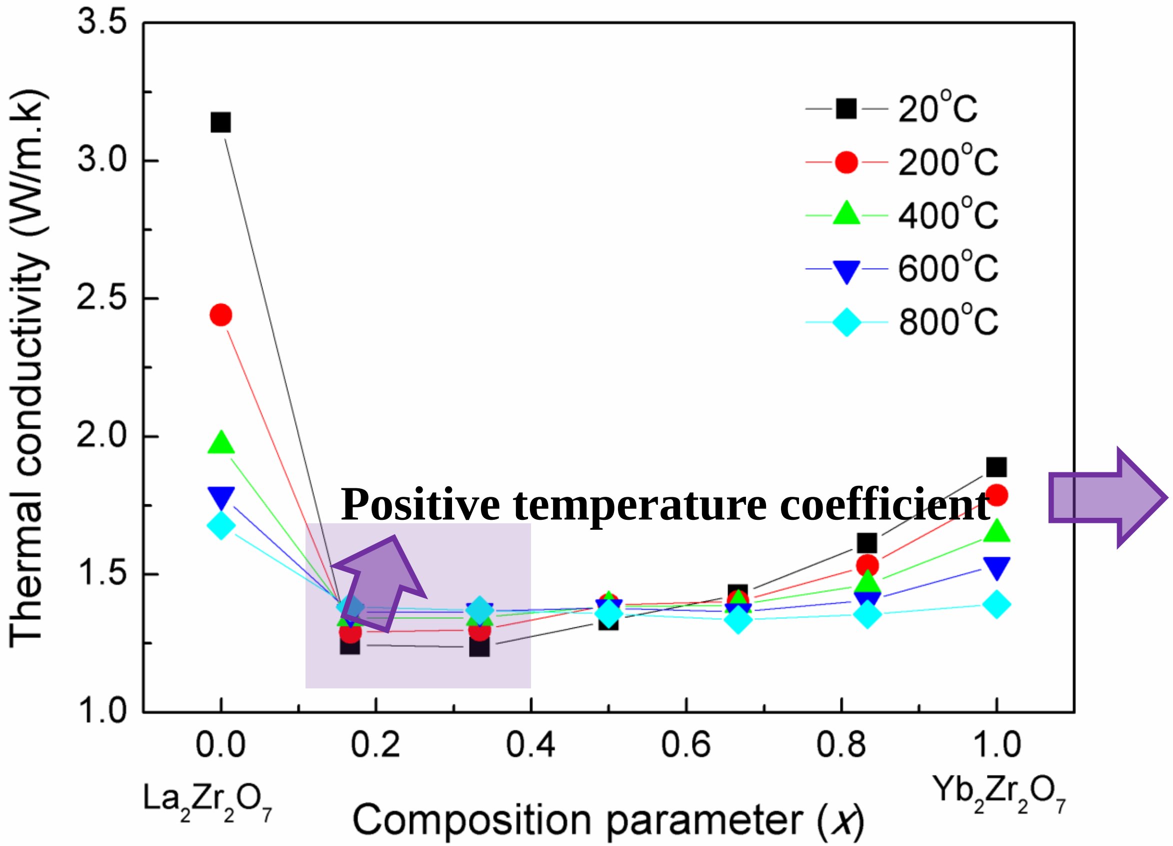

Glass-like

Wan CL, et al. *Acta Mater.*, 58, 6166–6172, (2010).

“Alloying limit” vs “Amorphous limit”

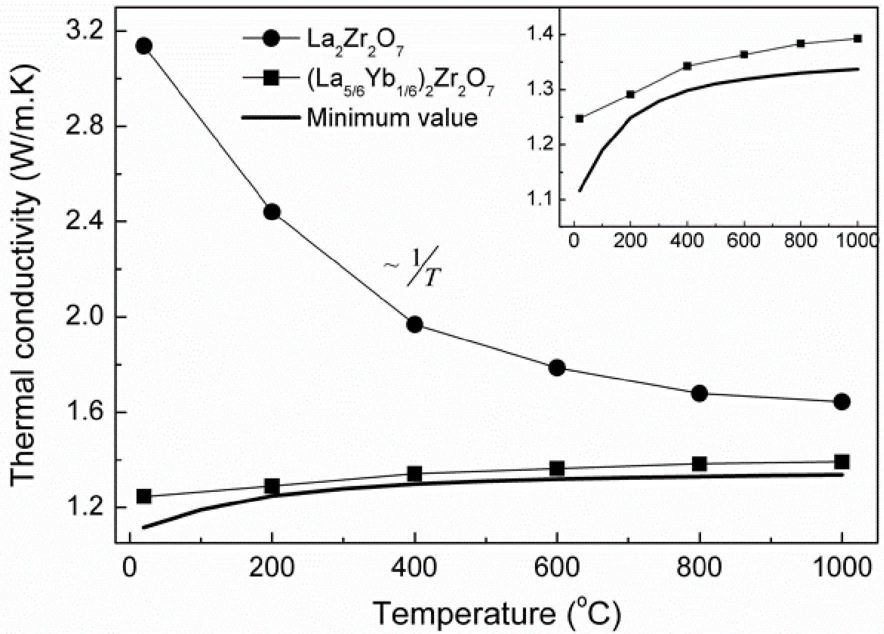

Minimum thermal conductivity

$$\Lambda_{\min} = \left(\frac{\pi}{6}\right)^{1/3} k_B n^{2/3} \sum_i v_i \left(\frac{T}{\theta}\right)^2 \int_0^{\theta_i/T} \frac{x^3 e^x}{(e^x - 1)^2} dx$$

$$\theta_i = v_i \left(\hbar / k_B\right)\left(6\pi^2 n\right)^{1/3}$$

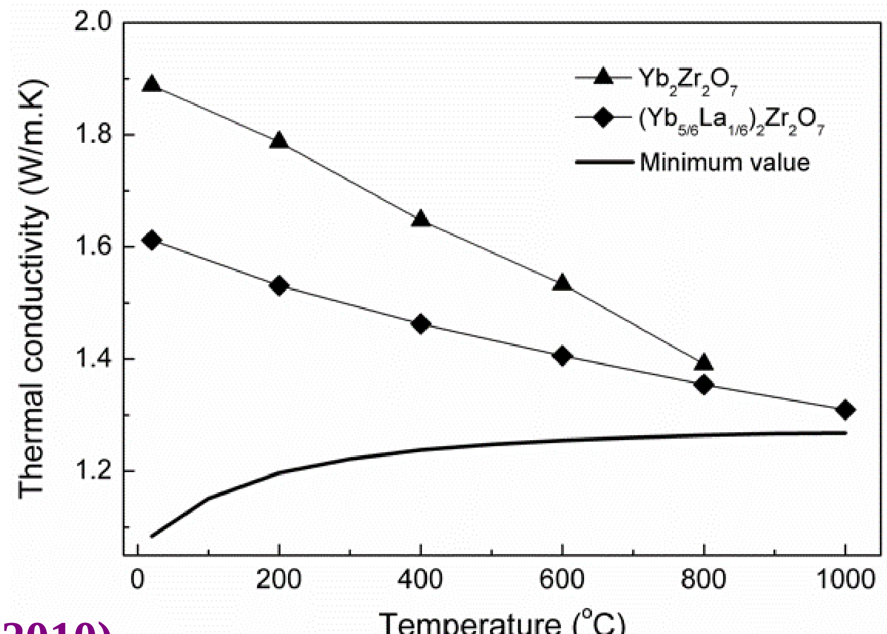

Amorphous limit

Alloying limit

Wan CL, et al. *Acta Mater.*, 58, 6166–6172, (2010).

$(La_{1-x}Yb_x)_2Zr_2O_7$- microstructure

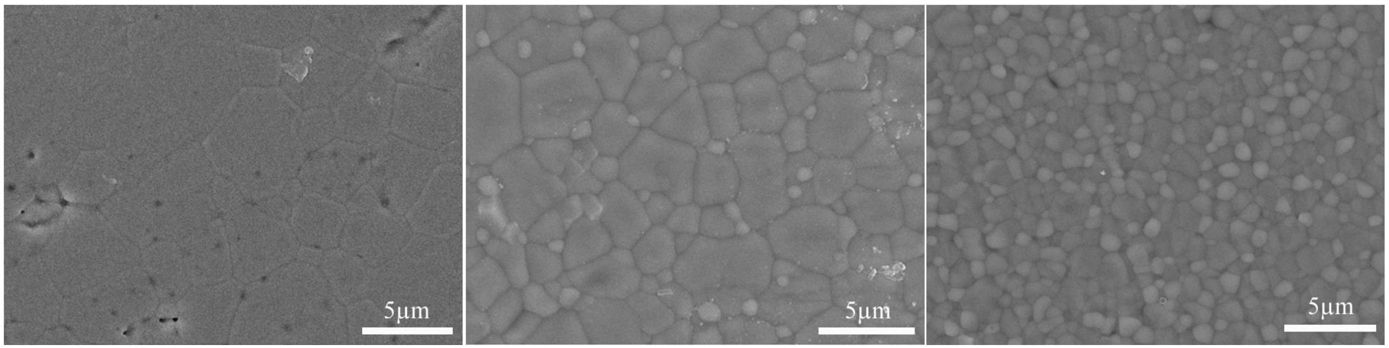

X=0 ($La_2Zr_2O_7$) X=1/6 X=1/3

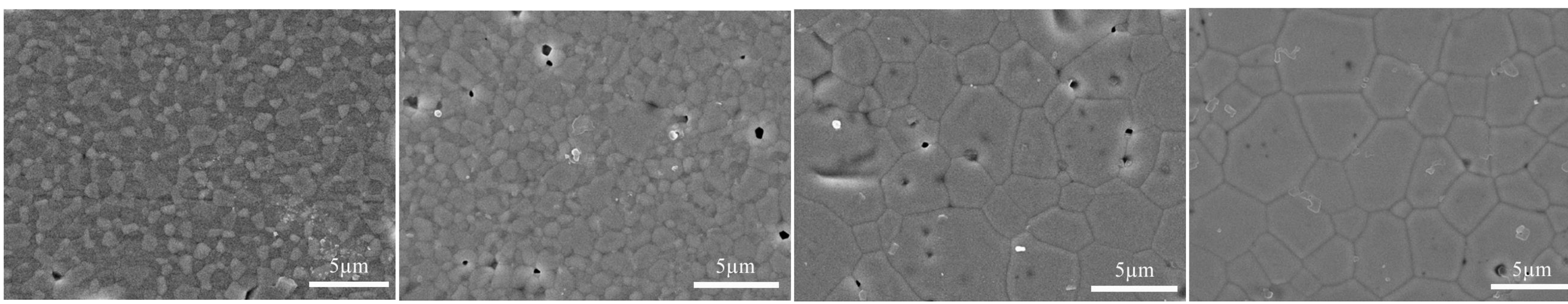

X=1/2 X=2/3 X=5/6 X=1 ($Yb_2Zr_2O_7$)

Surface morphology of $(La_{1-x}Yb_x)_2Zr_2O_7$ after annealing at 1600°C for 20hours

$(La_{1-x}Yb_x)_2Zr_2O_7$-toughness

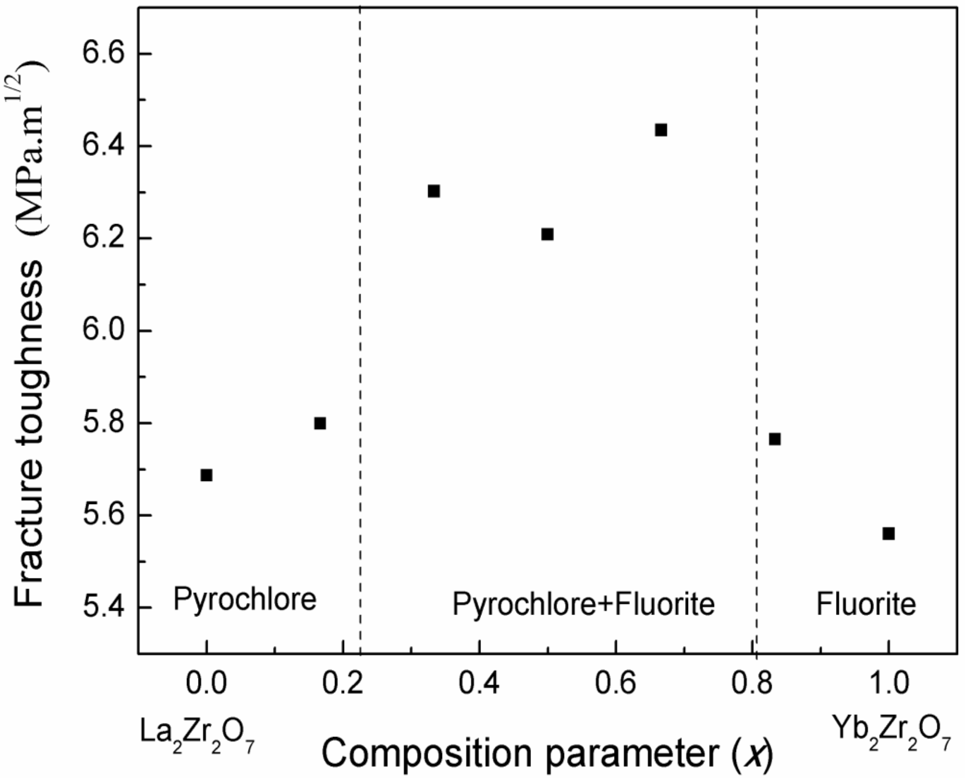

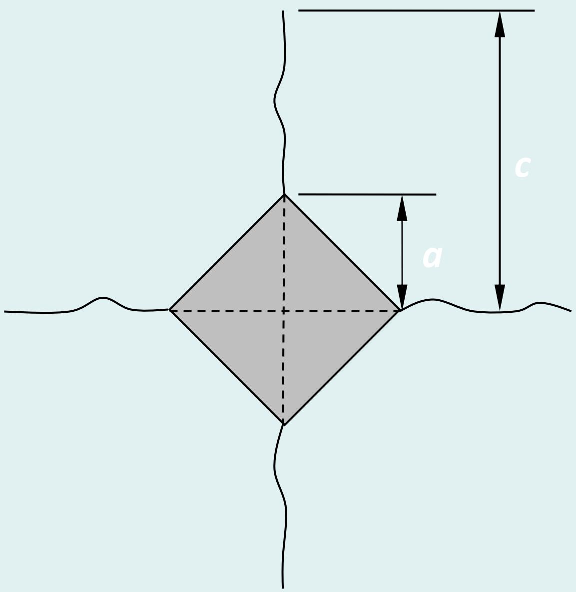

$$K_C = \alpha \left(\frac{E}{H} \right)^{1/2} \left(\frac{P}{c^{3/2}} \right)$$

Toughness measured by indentation method

Order-disorder Transition in Solid Solutions with A site doping in $A_2B_2O_7$

$(Sm_{1-x}Yb_x)_2Zr_2O_7$

CL wan, et al, J. Am. Ceram. Soc., 94 [2] 592–596 (2011).

Order-disorder transition in $(Sm_{1-x}Yb_x)_2Zr_2O_7$

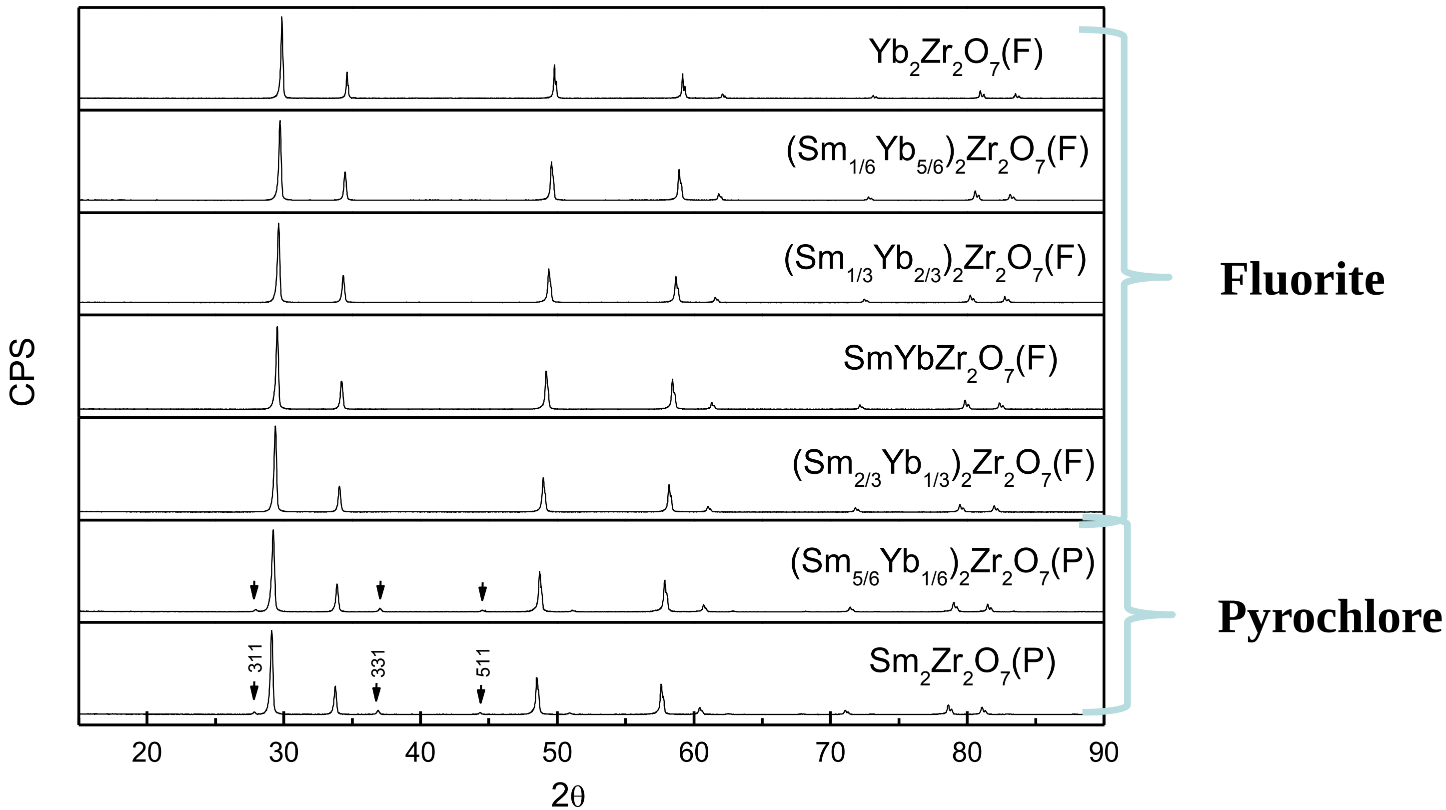

XRD pattern

CL wan, et al, J. Am. Ceram. Soc., 94 [2] 592–596 (2011).

Raman spectral analysis

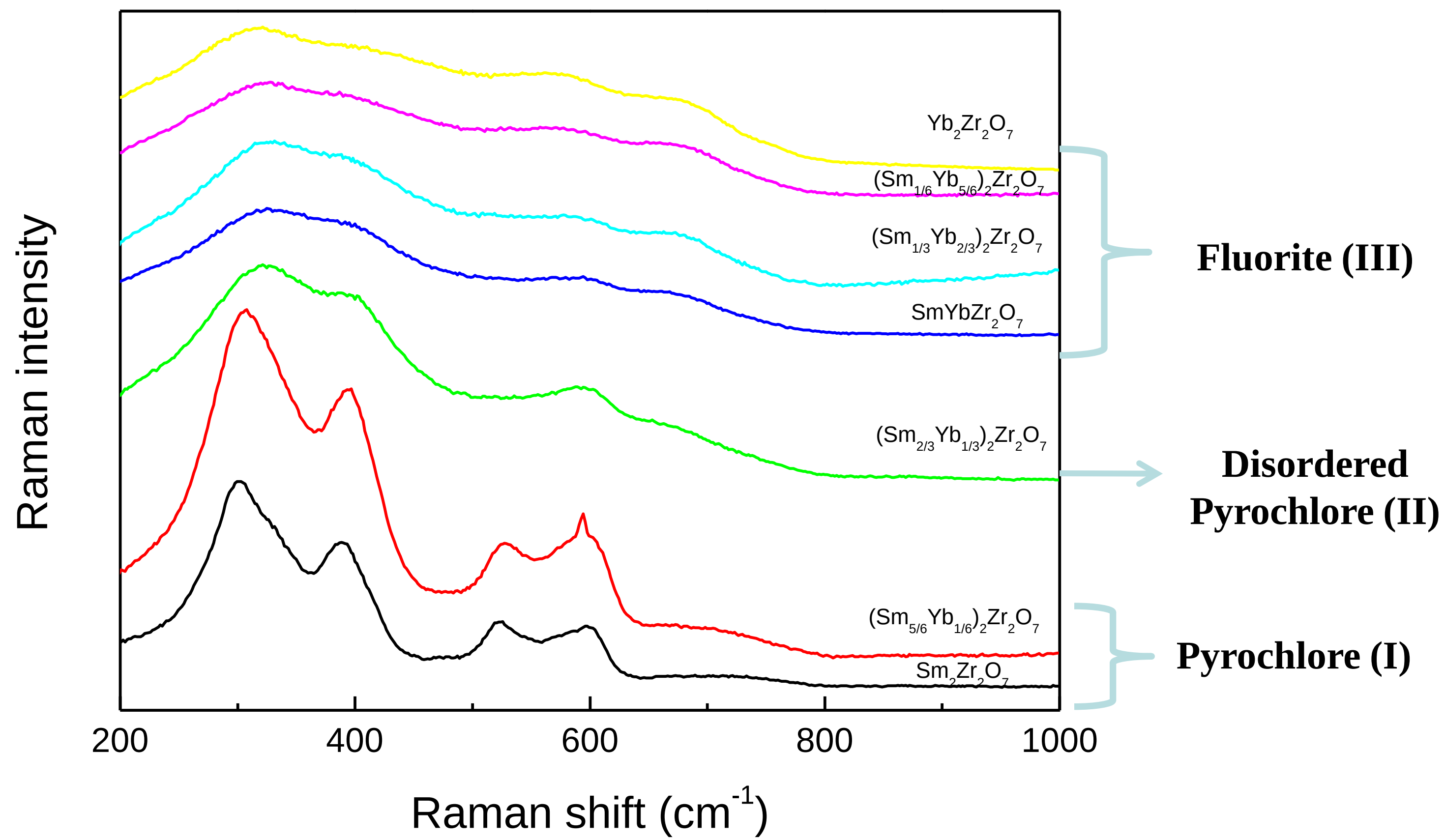

CL wan, et al, J. Am. Ceram. Soc., 94 [2] 592–596 (2011).

Young's modulus of $(Sm_{1-x}Yb_x)_2Zr_2O_7$

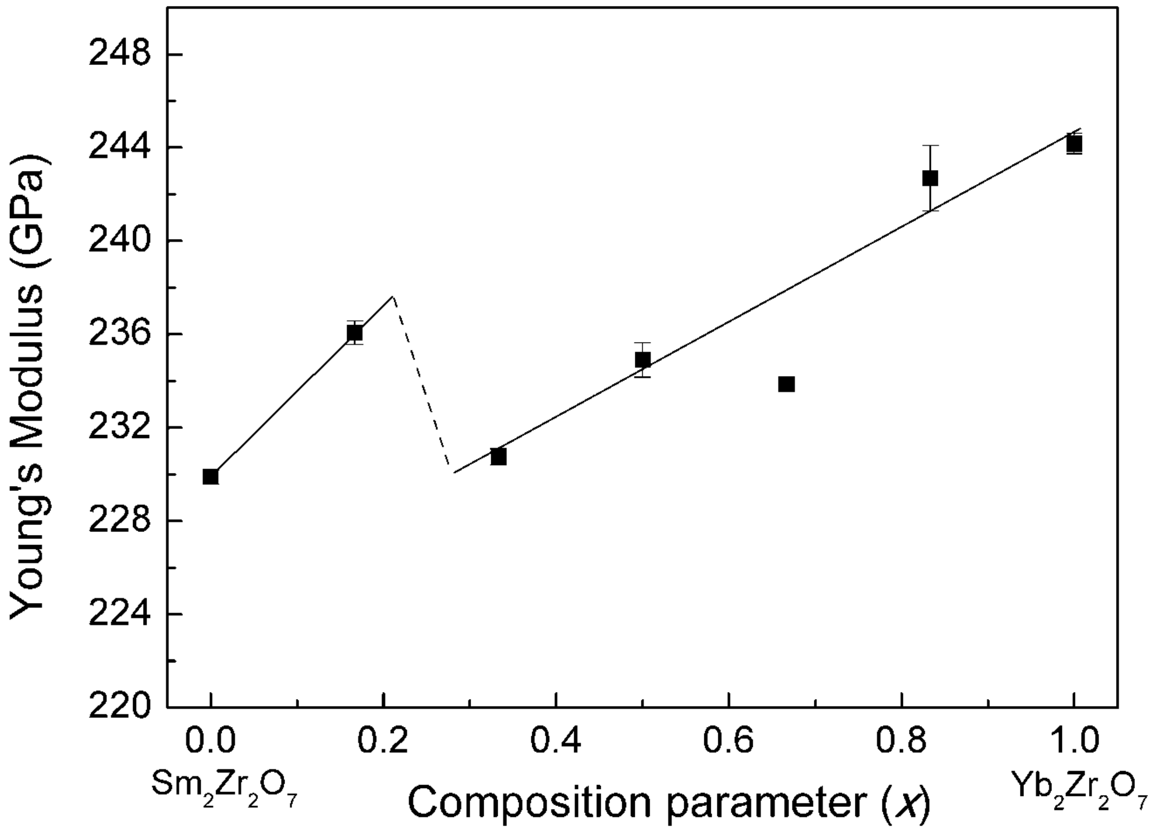

CL wan, et al, J. Am. Ceram. Soc., 94 [2] 592–596 (2011).

Thermal conductivity of $(Sm_{1-x}Yb_x)_2Zr_2O_7$

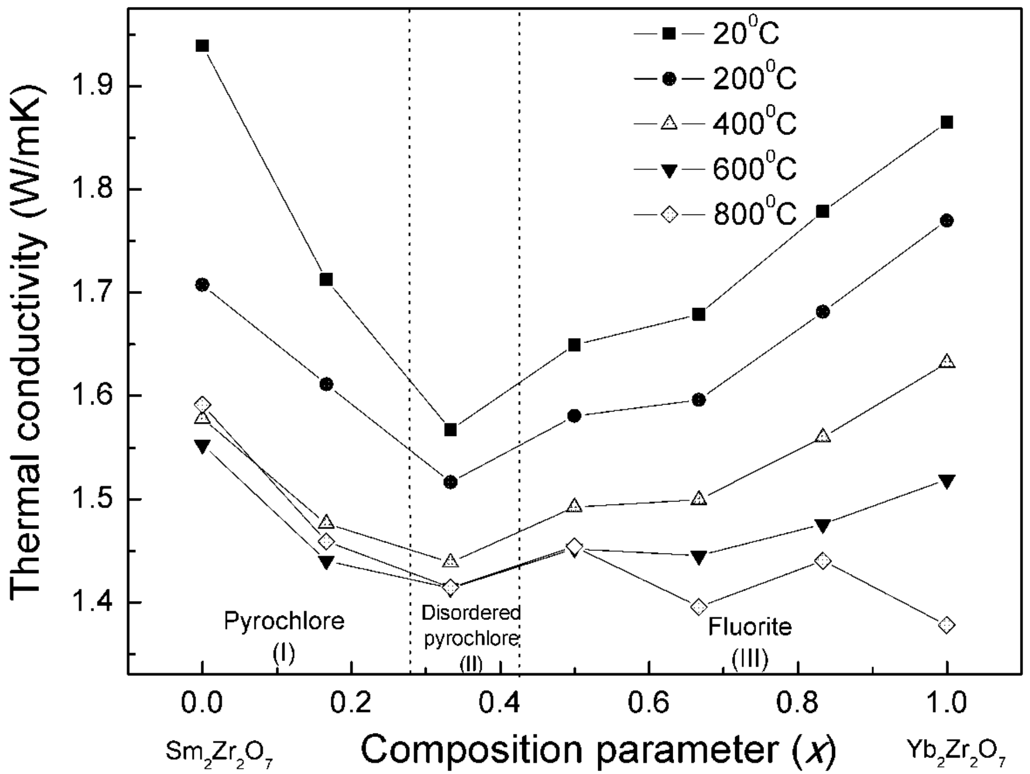

CL wan, et al, J. Am. Ceram. Soc., 94 [2] 592–596 (2011).

Vacancy, substitution and interstitial
TiO_2-doped YSZ

Ti doping YSZ (substitution + interstitial)

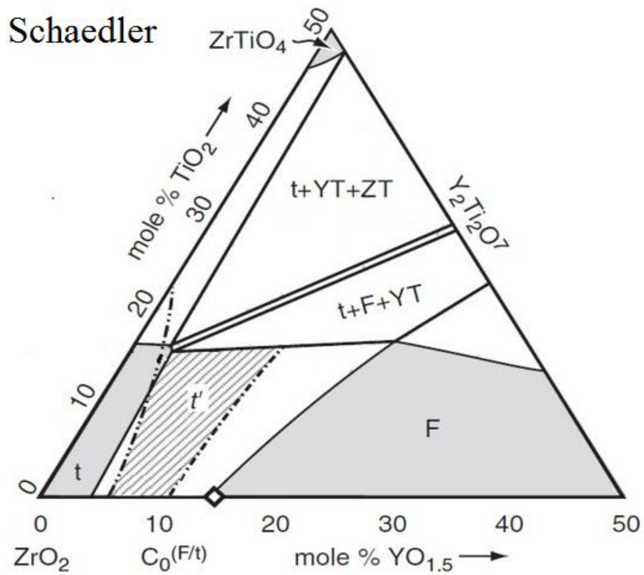

Schaedler TA, et al. *J Am Ceram Soc 2007;90:3896*.

No oxygen vacancy is introduced when Ti^{4+} substituting Zr^{4+}.

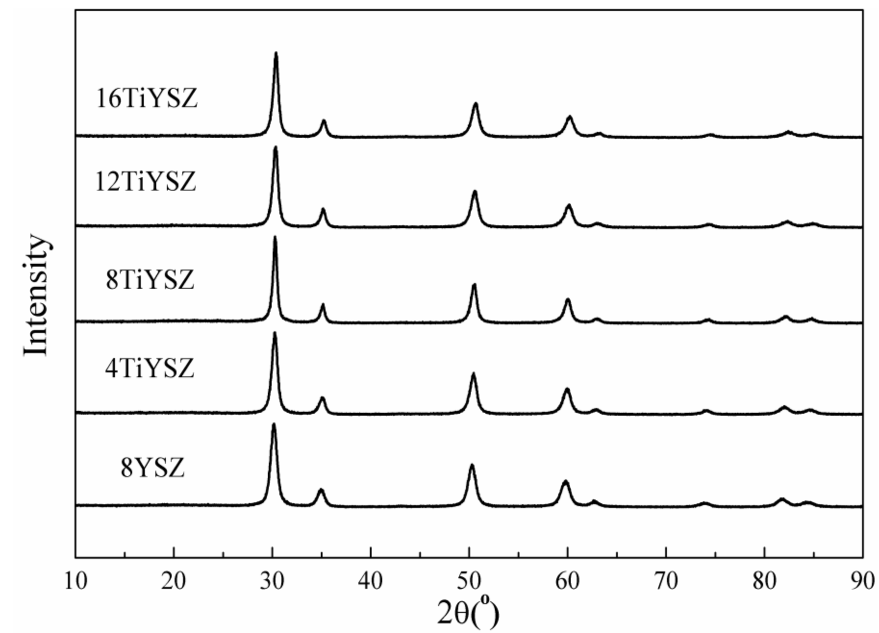

Merits

- **Stabilize the T-prime phase at high temperature.**
- **Enhance the ferroelastic toughening at high temperature.**

M. Zhao, W Pan, *Acta Mater., 61, 5496-5503(2013).*

Thermal conductivity of TiO_2-doped YSZ

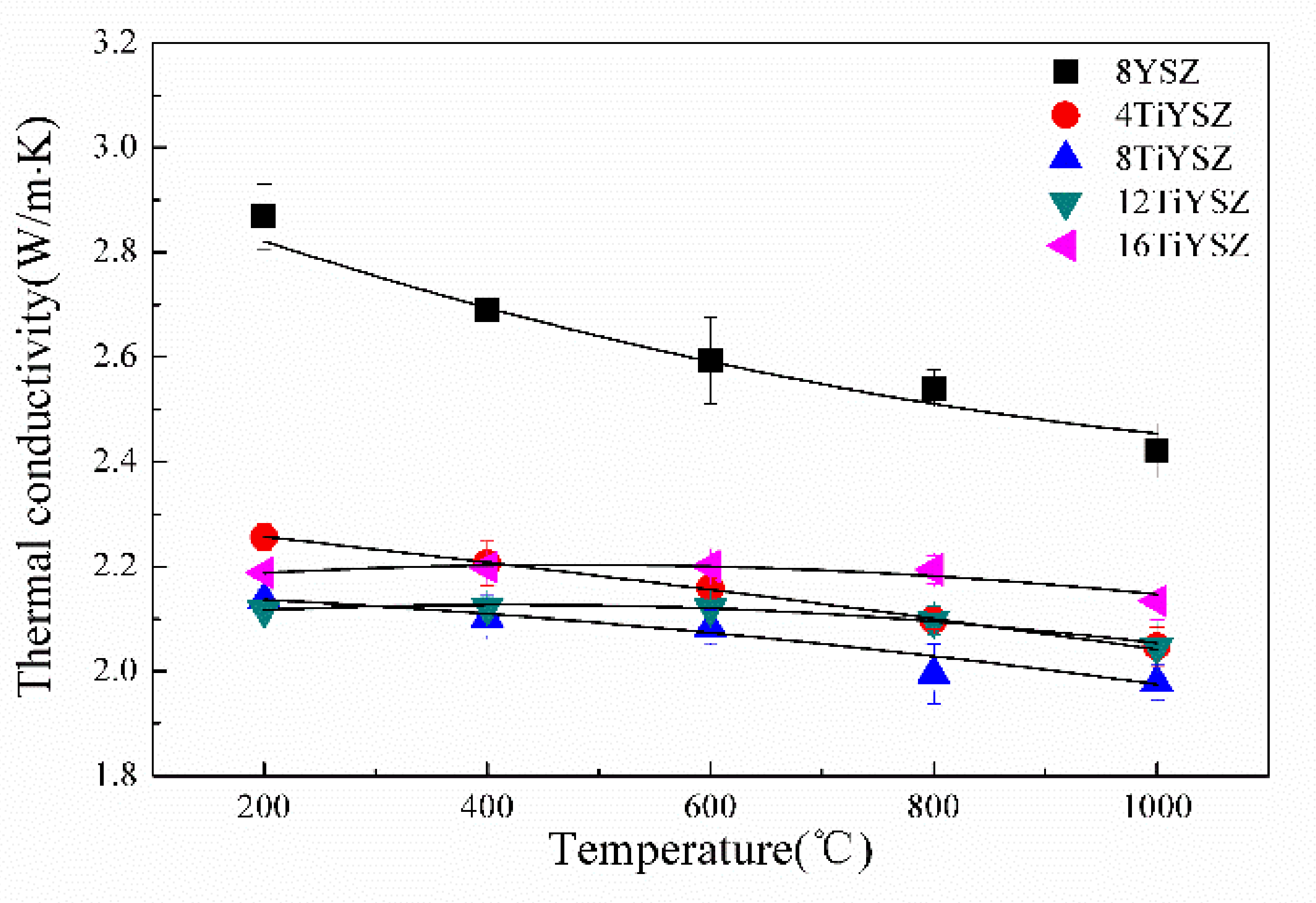

M. Zhao, W Pan, *Acta Mater., 61, 5496-5503(2013).*

Ti doping in YSZ (substitution + interstitial)

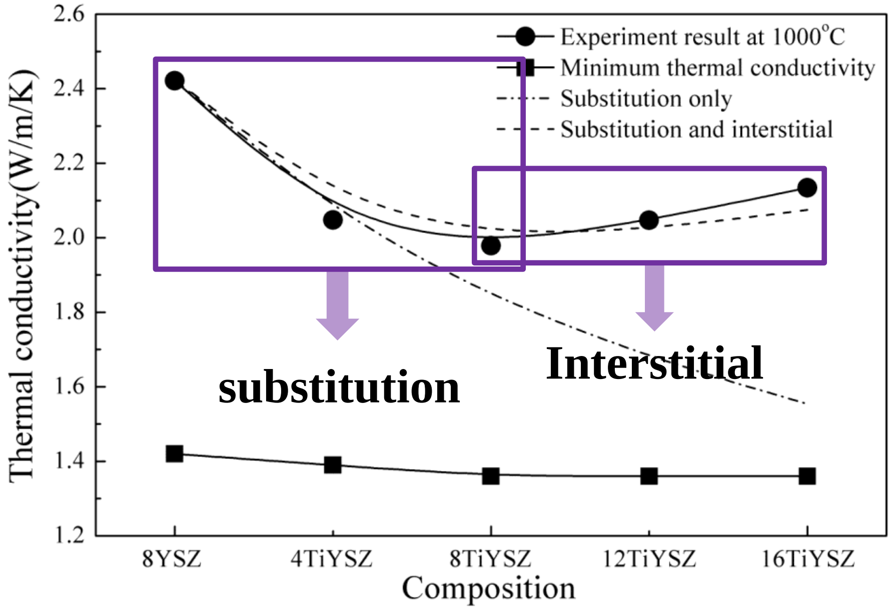

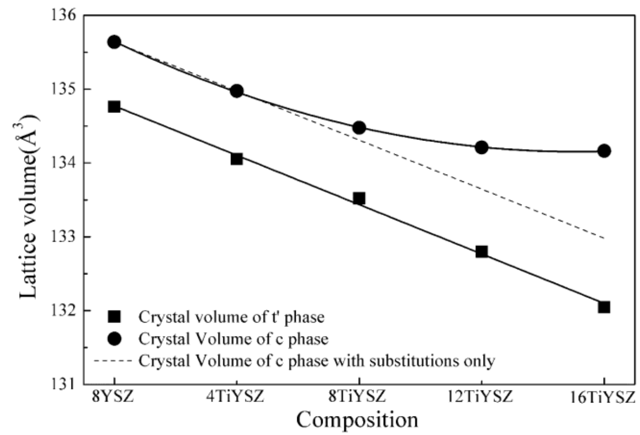

$$TiO_2 \xrightarrow{ZrO_2} Ti_{Zr}^{\times} + 2O_O^{\times}$$

$$TiO_2 \xrightarrow{ZrO_2} Ti_i^{4+} + 2O_i^{2-}$$

$$2O_i^{2-} + 2V_O^{2+} \longrightarrow 2O_O^{\times}$$

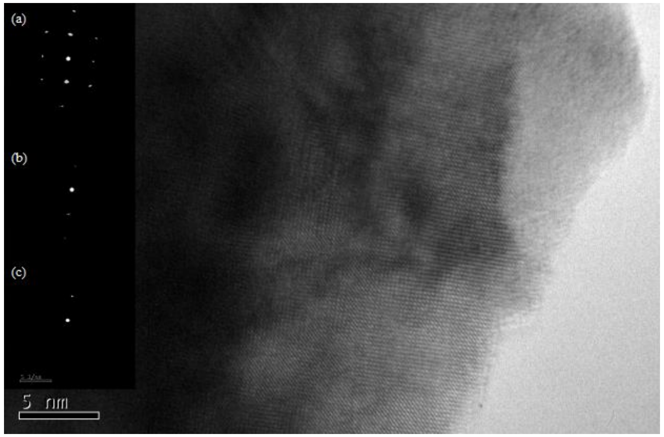

M. Zhao, W Pan, *Acta Mater.*, 61, 5496-5503(2013).

Complex Structure Oxides

$RE_{9.33+x}(SiO_4)_6O_{2+3x/2}$

Low modulus and large molecular weight

Material	Young's modulus (GPa)	Sound speed (m/s)
7YSZ	250.0	4326
$Gd_2Zr_2O_7$	234.3	3832
$La_{9.33}Si_6O_{26}$	140.3	3547
$Nd_{9.33}Si_6O_{26}$	141.6	3415
$Sm_{9.33}Si_6O_{26}$	143.5	3348
$Gd_{9.33}Si_6O_{26}$	148.5	3311

Ruifen Wu, Wei Pan et al. *Acta Mater.*, 60, 5536–5544(2012).

Defects in $RE_{9.33+x}(SiO_4)_6O_{2+3x/2}$ with apatite structure

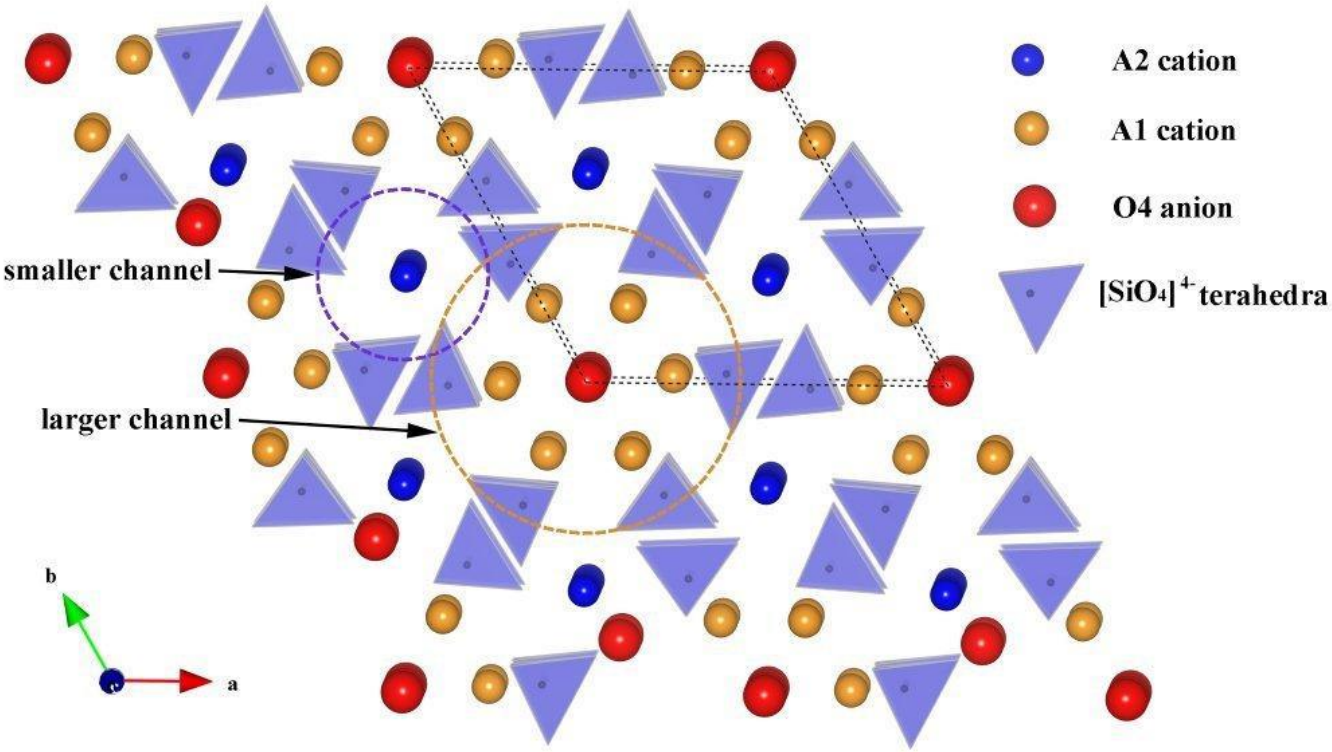

Two types of defects

Ruifen Wu, Wei Pan et al. *Acta Mater.*, 60, 5536–5544(2012).

Thermal conductivity of $RE_{9.33+x}(SiO_4)_6O_{2+3x/2}$

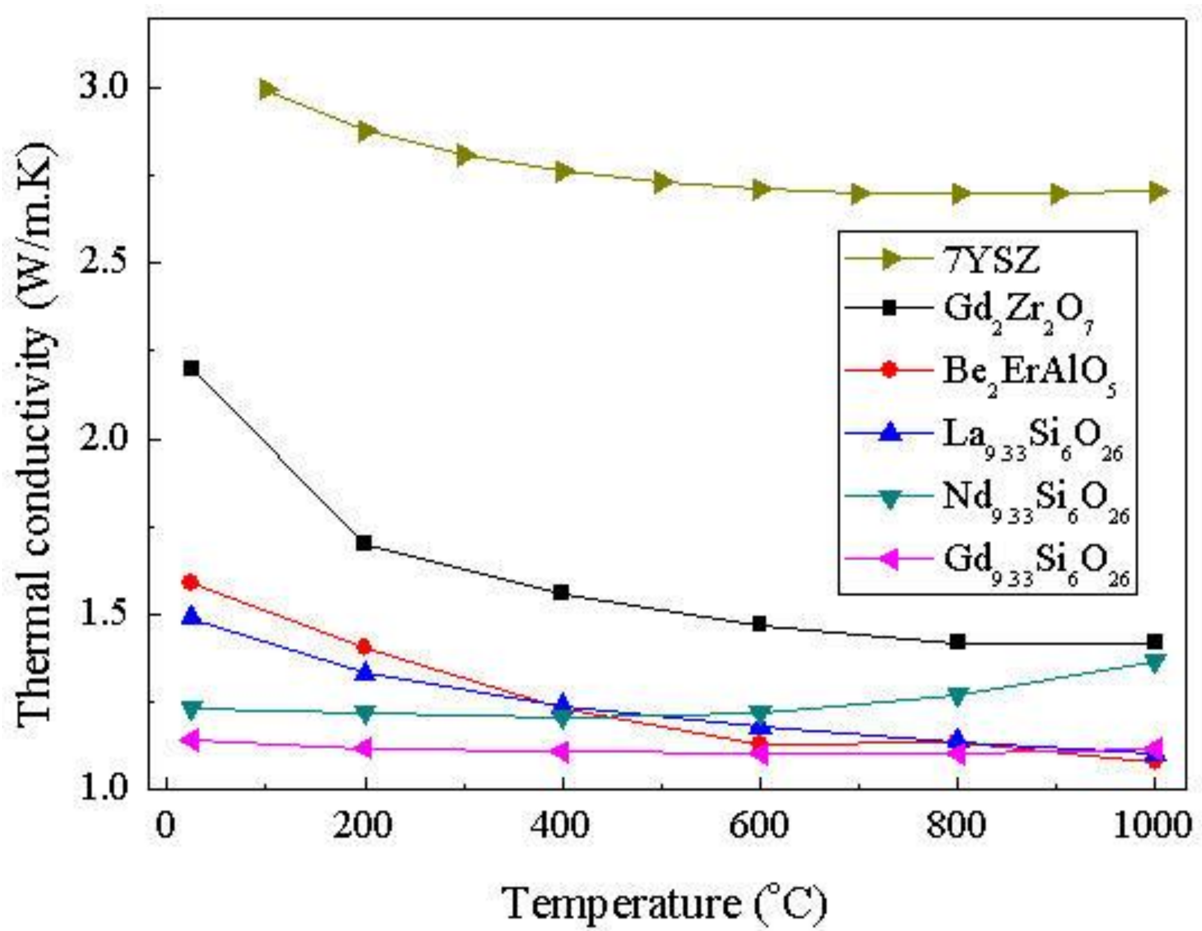

Extremely low!
κ=1.1W/m/K

Ruifen Wu, Wei Pan et al. *Acta Mater.*, 60, 5536–5544(2012).

Thermal conductivity in anisotropy oxides

Textured $LaPO_4$ with Monazite structure

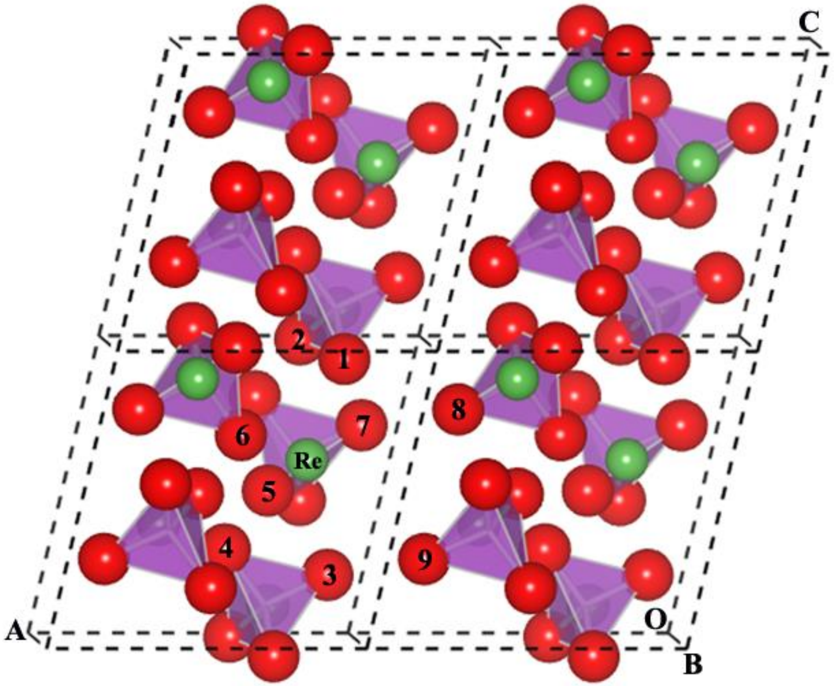

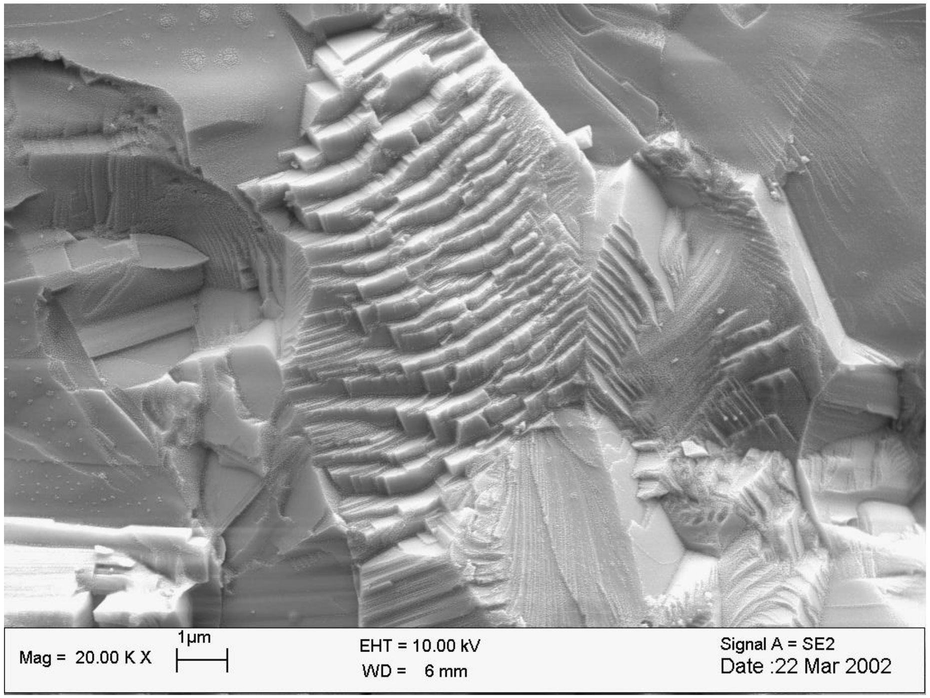

AB Du, W Pan. *J. Am. Ceram. Soc.*, 92[11], 2687–2692(2009).

Texture controlled by processing

Different textured $LaPO_4$ oxides prepared with controlled sintering process.

$$\alpha = S(200)/S(120)$$

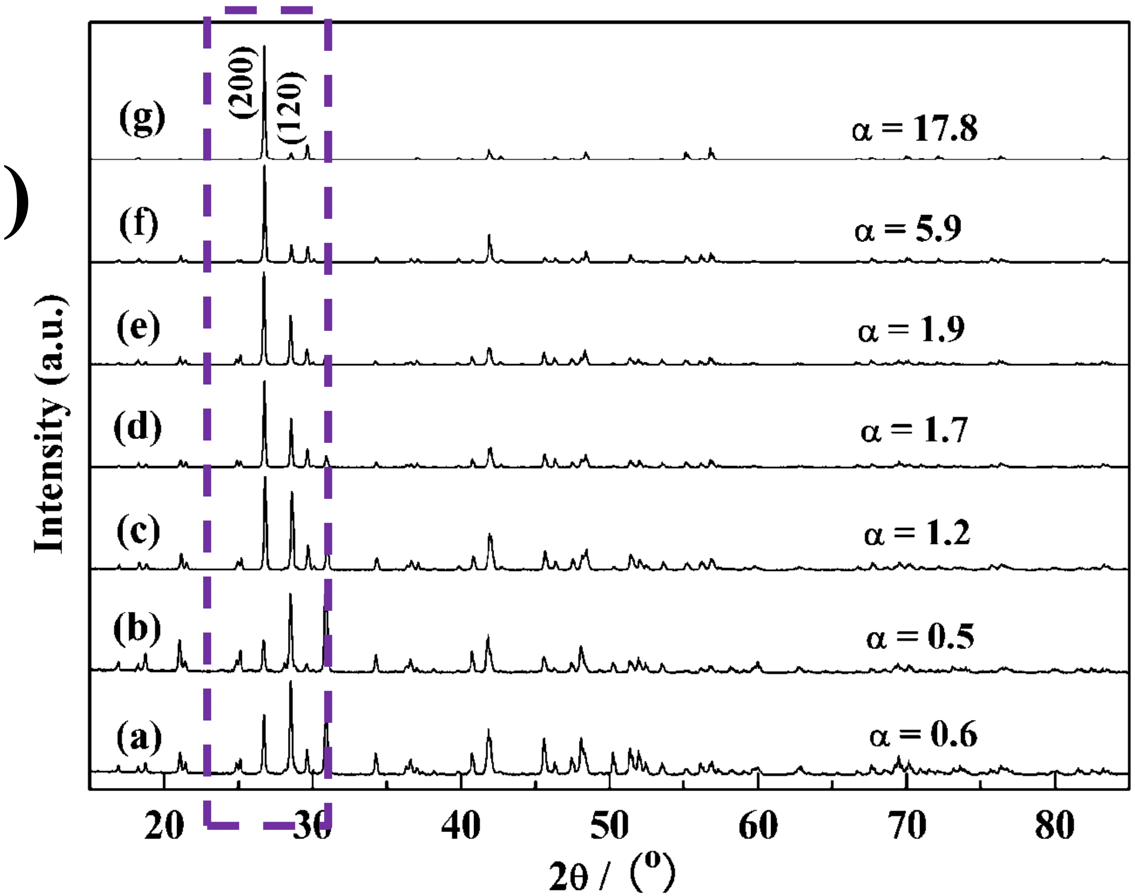

AB Du, W Pan. *J. Am. Ceram. Soc.*, 92[11], 2687–2692(2009).

Thermal Conductivity of the Textured $LaPO_4$

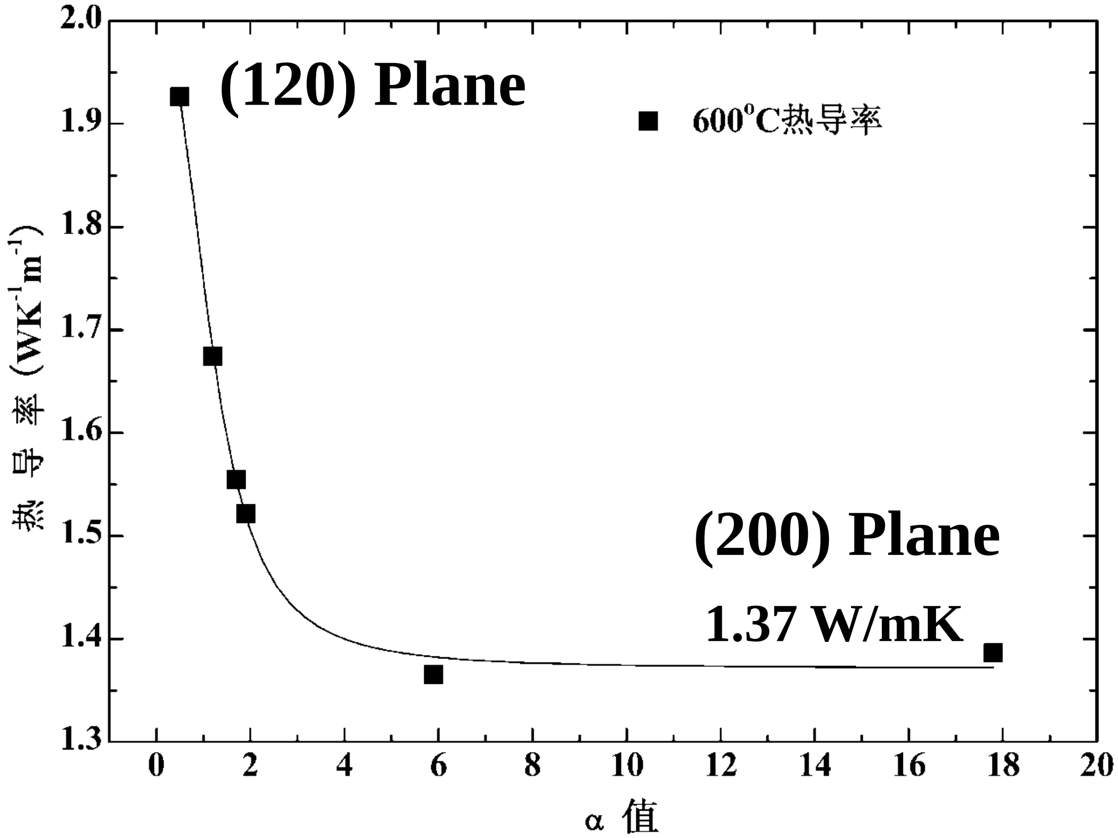

$$k = 1.372 + \frac{0.616}{1 + \left(\frac{\alpha}{1.197}\right)^{2.511}}$$

AB Du, W Pan. *J. Am. Ceram. Soc.*, 92[11], 2687–2692(2009).

Thermal Conductivity of the $RE_2SrAl_2O_7$

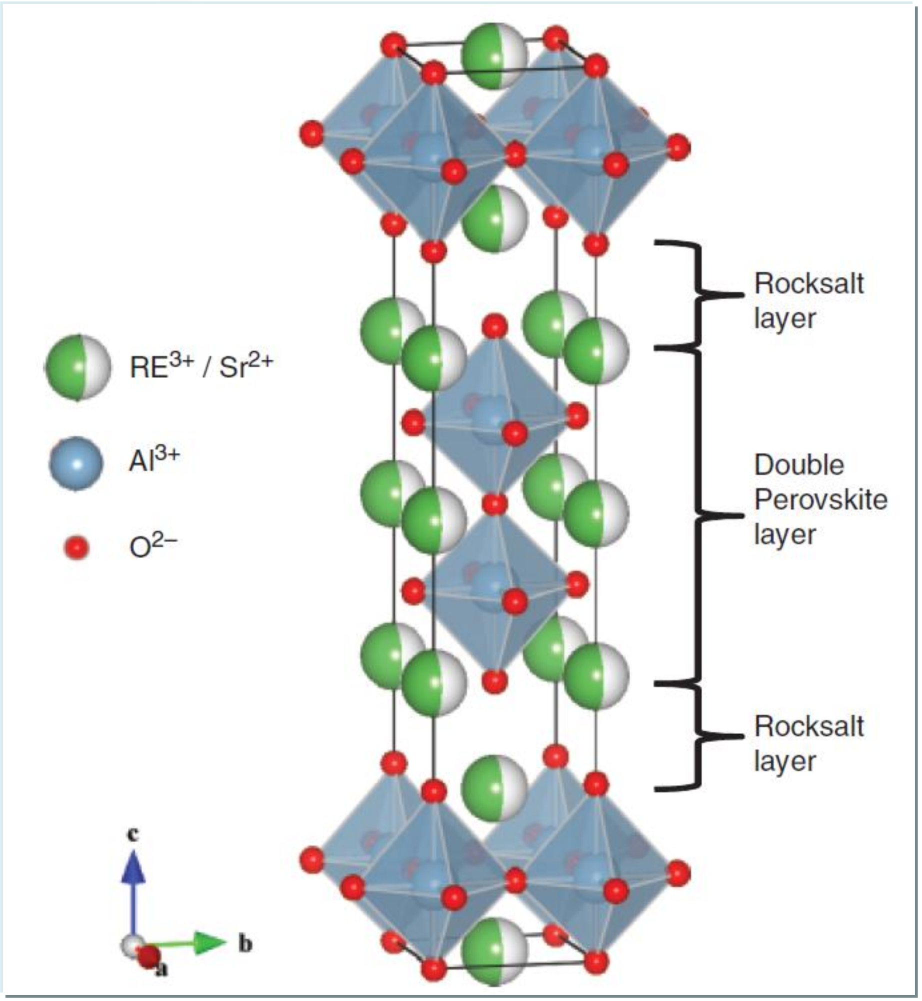

$RE_2SrAl_2O_7$

RE=Sm, Eu, Gd, Dy

CL Wan, TD Sparks, W Pan, DR Clarke. *J. Am. Ceram. Soc.*, 93[5], 1457–1460(2010).

Thermal Conductivity of the $RE_2SrAl_2O_7$

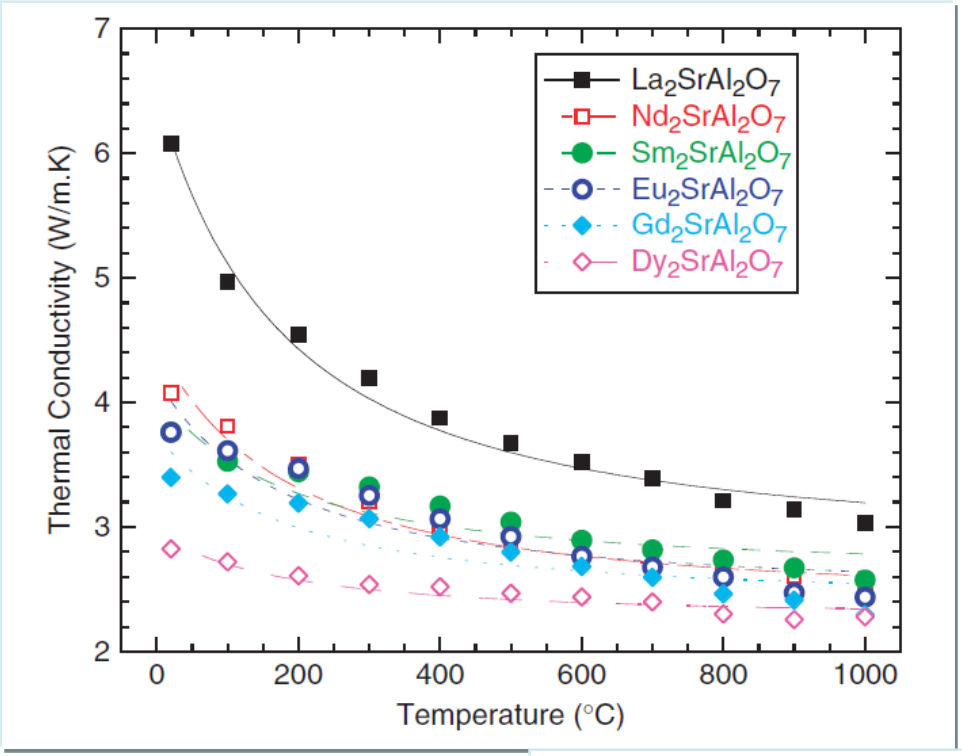

$$k = \frac{A}{T}\left[\frac{2}{3}\sqrt{\frac{T_1}{T}} + \frac{T}{3T_1}\right] = \frac{2A\sqrt{T_1}}{3T^{3/2}} + \frac{A}{3T_1}$$

CL Wan, TD Sparks, W Pan, DR Clarke. *J. Am. Ceram. Soc.*, 93[5], 1457–1460(2010).

Calculation by first principles and density functional perturbation theory (DFPT) method

Calculated using the first principlesand density functional perturbation theory(DFPT) method

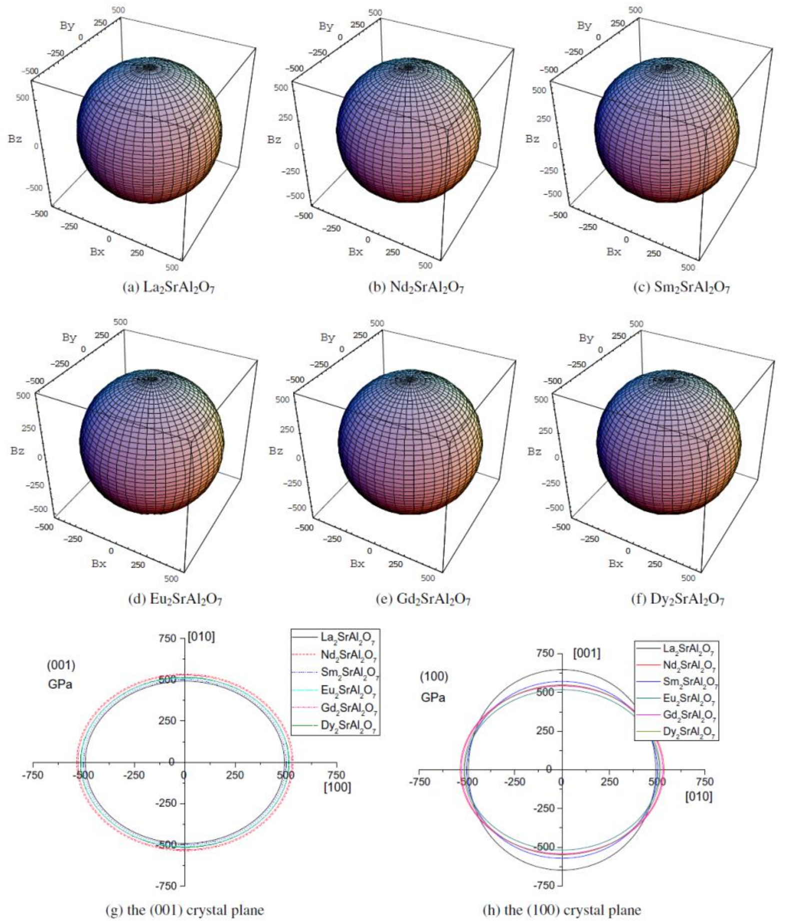

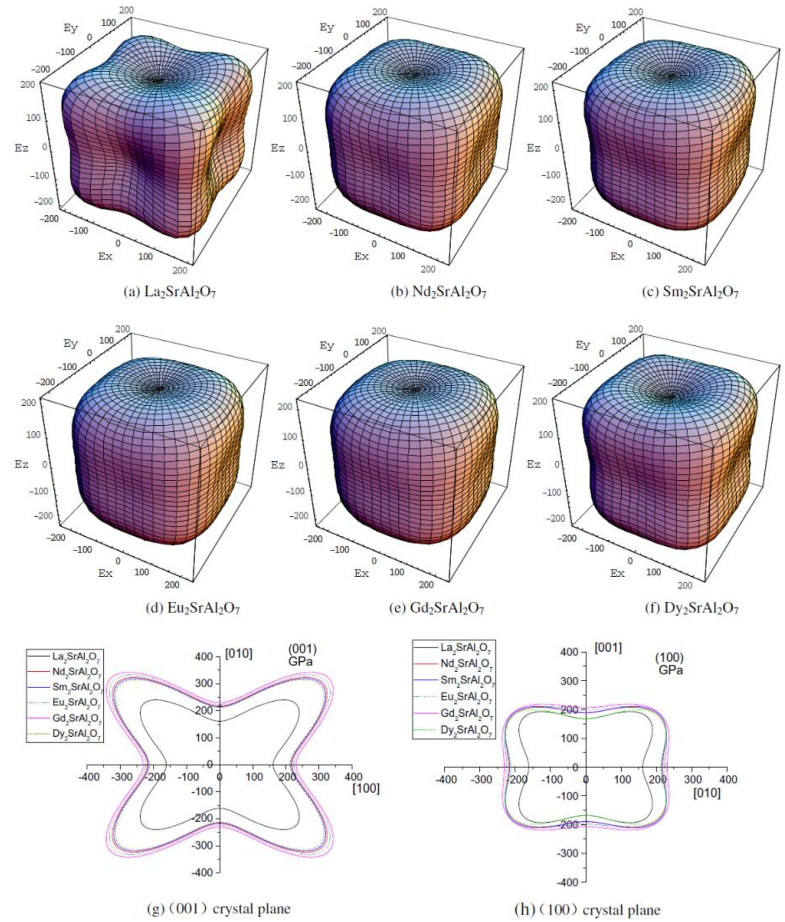

The calculations were supplemented using the quasi-harmonic approximation (QHA), and spin polarized local density approximation (LSDA)

Jing Feng, Wei Pan, *Acta Materialia*, 60, 3380–3392(2012).

Calculated thermal conductivity for different orientation

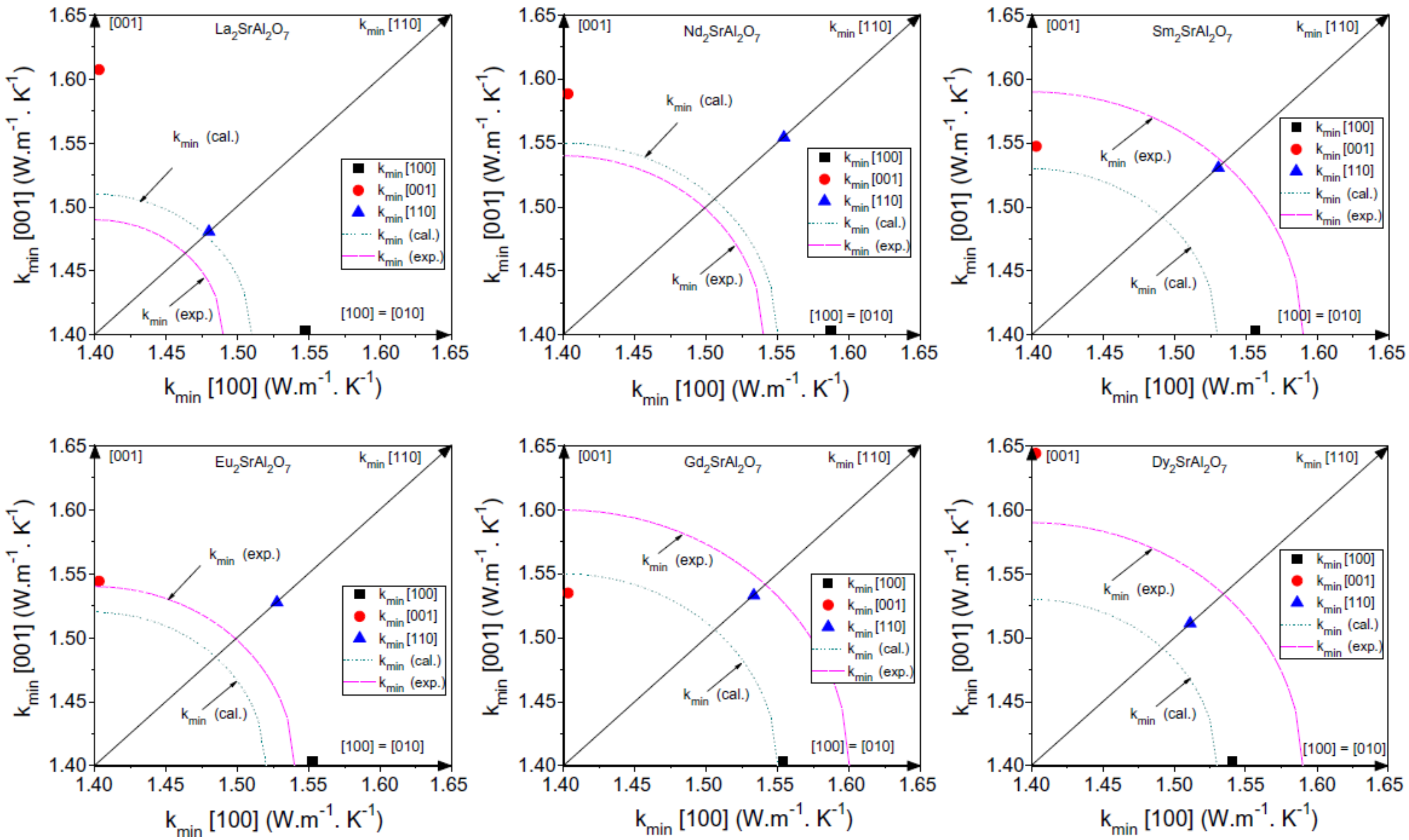

Jing Feng, Wei Pan, ***Acta Materialia*****, 60, 3380–3392(2012).**

Applications

Could pyrochlore $Sm_2Zr_2O_7$, $Gd_2Zr_2O_7$ oxides replace YSZ for TBC?

Spray TBCs by APS

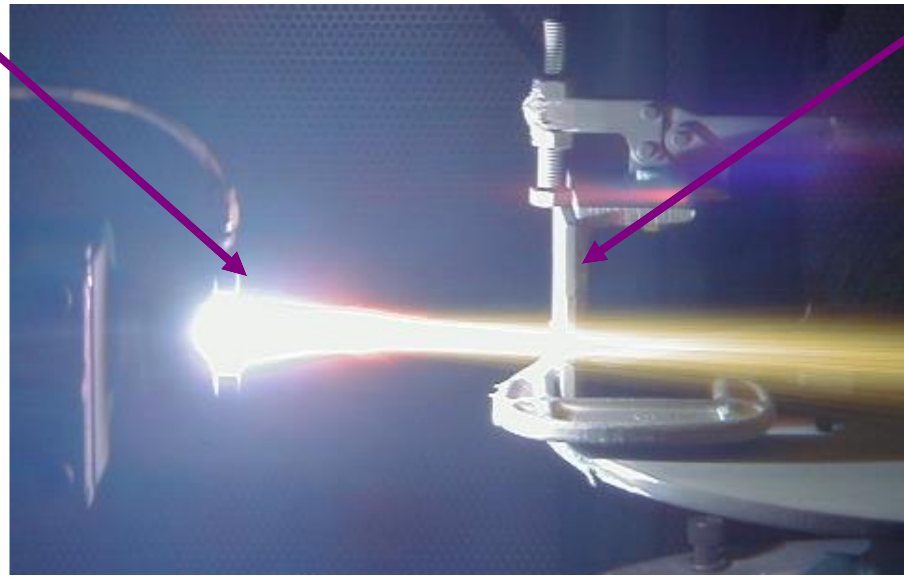

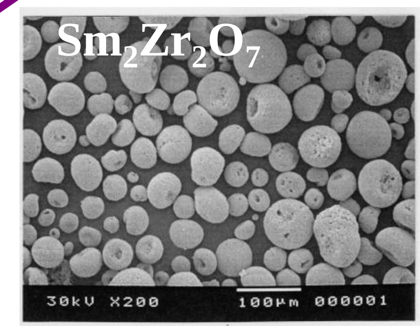

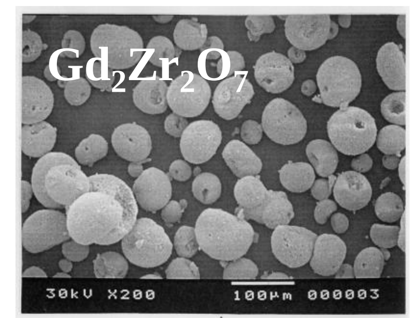

Spray condition①：（conventional)

Ar/H_2	35/7.4[l/min]
Current	600[A]
Spray distance	150[mm]
Supplying speed	60[g/min]

Spray condition②：

Ar/H_2	Same as ①
Current	500[A]
Spray distance	Same as ①
Supplying speed	Same as ①

Observation after the Spraying

Spray efficiency is equal to YSZ

(Spray condition ① ; YSZ：18μm/pass　$Sm_2Zr_2O_7$ ：24μm/pass）

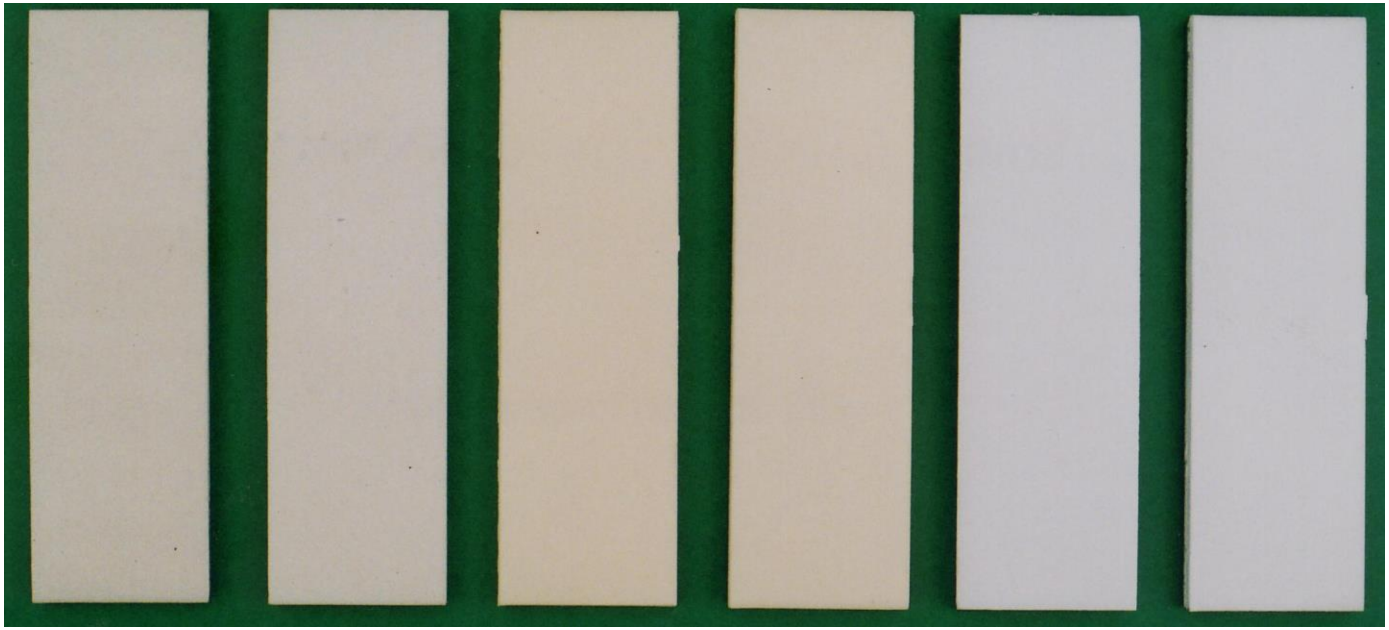

Spray condition ① ② ① ② ① ②

8YSZ　**$Sm_2Zr_2O_7$**　**$Gd_2Zr_2O_7$**

Observation of TBCs Cross Section

	YSZ	$Sm_2Zr_2O_7$	$Gd_2Zr_2O_7$
Spray condition①	Porosity：12.0% 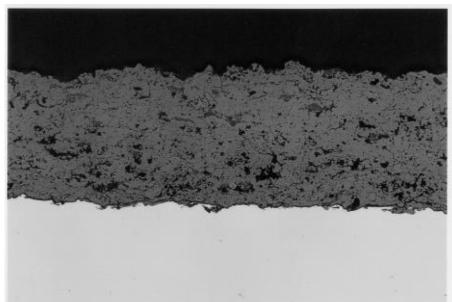	Porosity ：4.9% 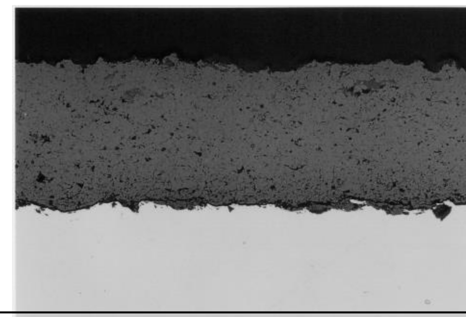	Porosity ：5.3% 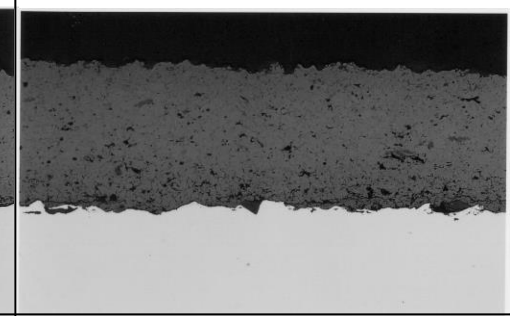
Spray condition②	Porosity ：11.8% 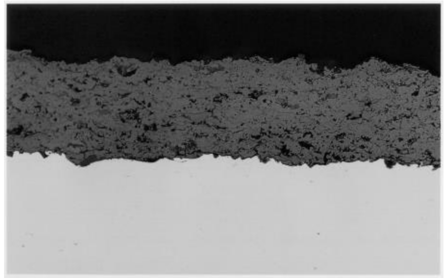	Porosity ：6.6% 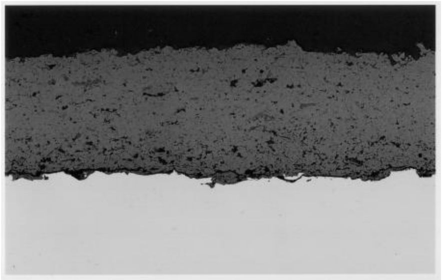	Porosity ：7.4% 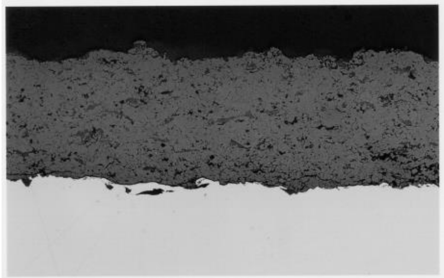

Estimation of the Thermal Conductivity

Radiation camera
(Measuring surface temperature,Ts)

CO_2 LASER nozzle

TBC specimen

CCD camera

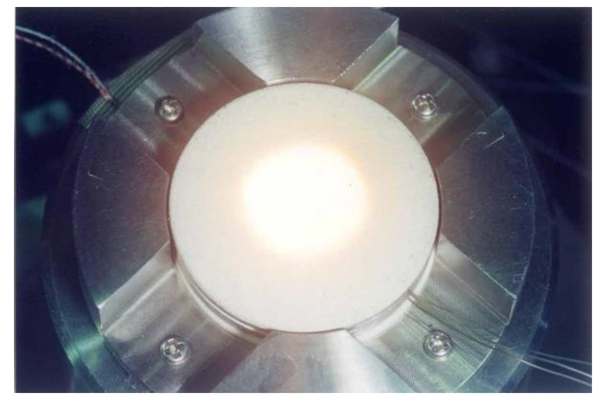

Cooling air

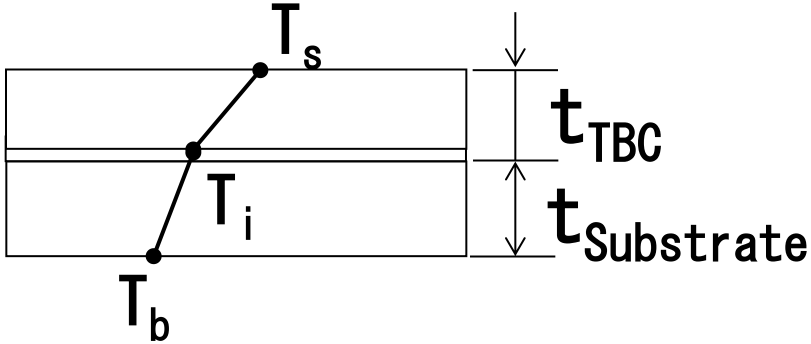

$$\lambda_2 = \lambda_1 \times \frac{(T_i - T_b)t_{substrate}}{(T_S - T_i)/t_{TBC}}$$

λ_1 : Substrate thermal conductivity
λ_2 : TBC thermal conductivity

Thermal conductivity of the Porous TBCs

Thermal conductivity of porous TBC($Sm_2Zr_2O_7$ and $Gd_2Zr_2O_7$)

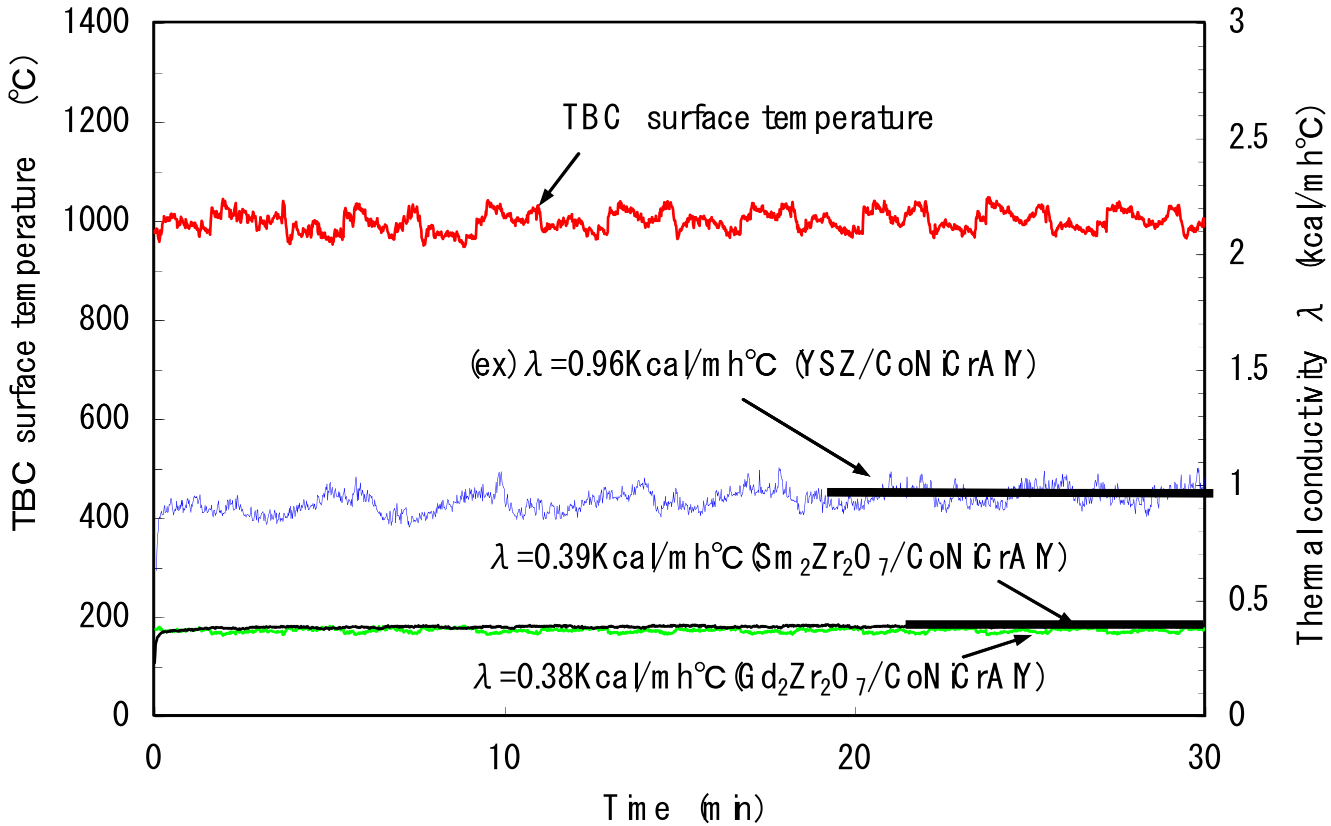

Bending test (Servo machine with SEM)

Specimen size

Spray　condition	YSZ	$Sm_2Zr_2O_7$	$Gd_2Zr_2O_7$
Spray condition　①	○	○	○
Spray condition　②		○	

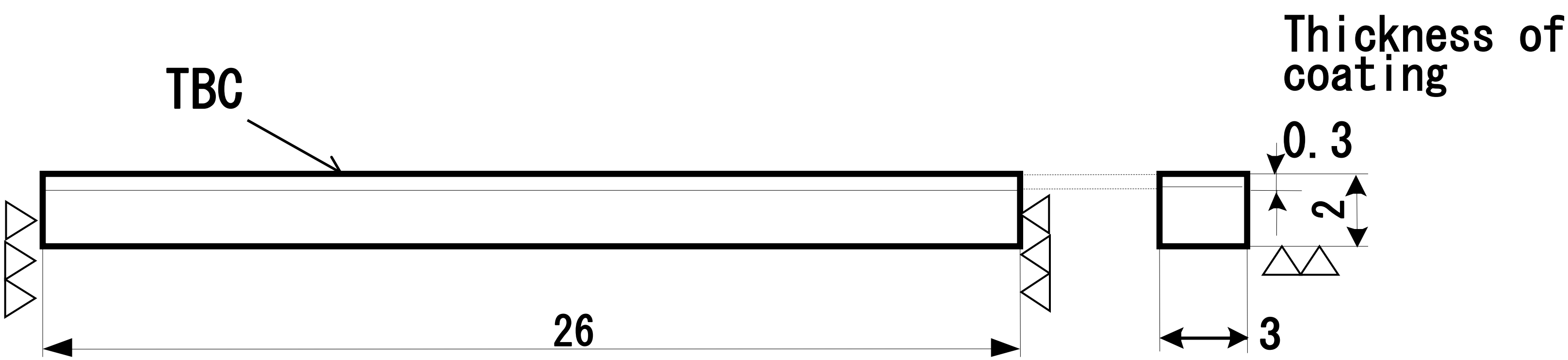

Bending test

- estimating the limit strain for vertical crack *
- The limit strain for vertical crack of $Sm_2Zr_2O_7$ is equal to conventional YSZ

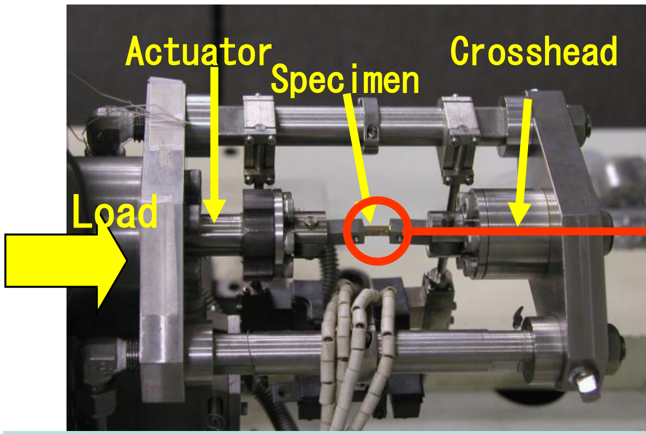

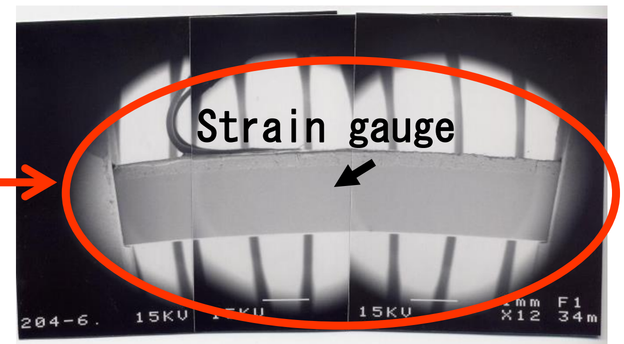

limit strain

YSZ	$Sm_2Zr_2O_7$	$Gd_2Zr_2O_7$
ε =0.35%	ε =0.32%	ε =0.22%

YSZ

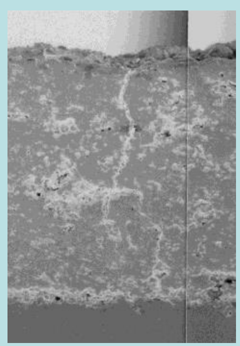

$Sm_2Zr_2O_7$

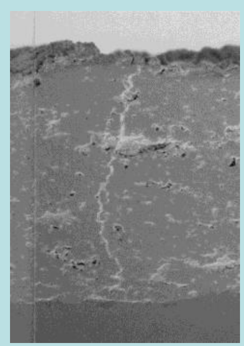

$Gd_2Zr_2O_7$

Spray condition ①

ε =0.38%

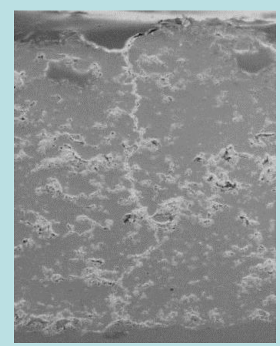

$Sm_2Zr_2O_7$

Spray condition②

Estimation for Bending strength

The limit strain of vertical crack of $Sm_2Zr_2O_7$ is equal to conventional YSZ

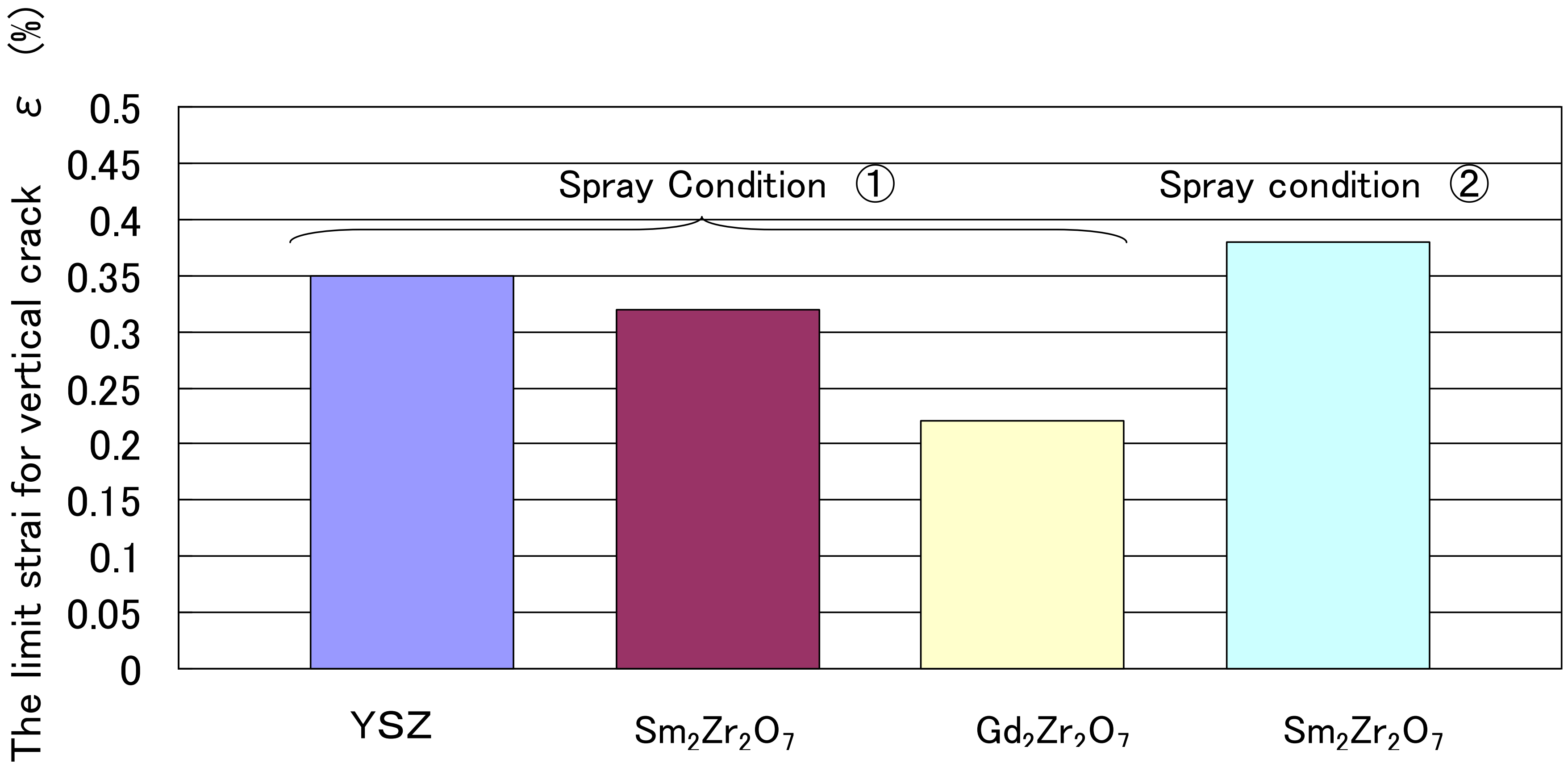

Thermal cycle results for flat plate specimen

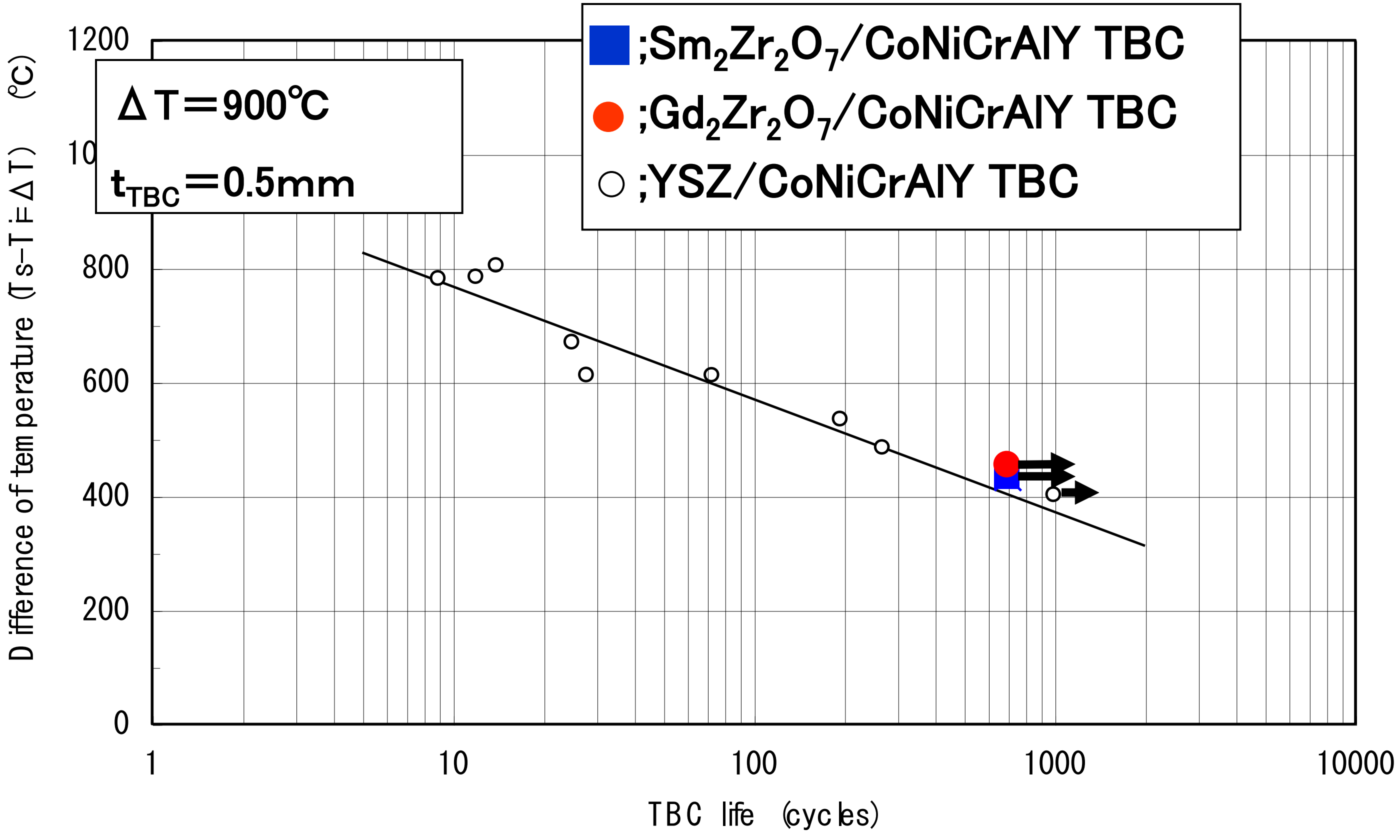

Ts ： TBC surface temperature

Tb ： TBC / substrate interface temperature

Thermal cycle results for cylindrical specimen

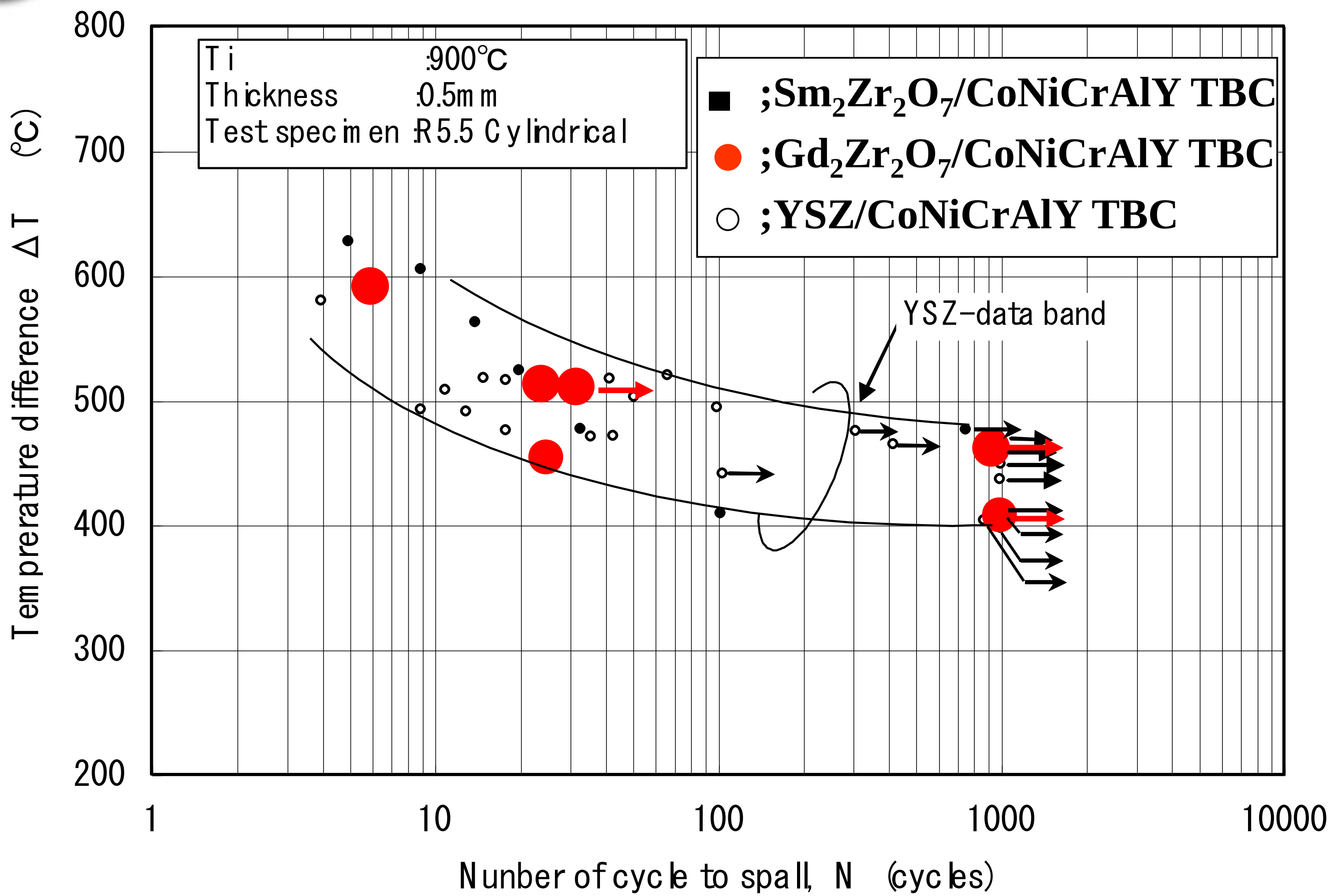

Acknowledgements to contributors

Tsinghua University: Chunlei Wan, Jing Feng, Zhixue Qu, Ruifen Wu, Xiaorui Ren, Meng Zhao

Harvard University: David R. Clarke, Taylor D. Sparks

University of Florida : Simon R. Phillpot, Aleksandr Chernatynskiy

Publications on TBCs

1. M Zhao, *W Pan*, Effect of lattice defects on thermal conductivity of Ti-doped, Y_2O_3-stabilized ZrO_2, *Acta Mater. 61 (2013) 5496–5503.*
2. RF Wu, *W Pan*, XR Ren, CL Wan, ZX Qu, AB Du, An Extremely Low Thermal Conductive Ceramic: $RE_{9.33}(SiO_4)_6O_2$ Silicate Oxyapatite, *Acta Mater. 60 (2012) 5536–5544.*
3. J. Feng, B. Xiao, R. Zhou, *W. Pan*, David R. Clarke, Anisotropic Mechanical and Thermal Properties of Double Perovskite Slab-Rocksalt Layer $Ln_2SrAl_2O_7$ (Ln = La, Nd, Sm, Eu, Gd and Dy), *Acta Mater. 60 (2012) 3380–3392.*
4. ZX Qu, CL Wan, *W Pan*, Thermophysical Properties of Rare-earth Stannates: Effect of Pyrochlore Structure, *Acta Mater. 60 (2012) 2939–2949.*
5. ZX Qu, Taylor Sparks, *W Pan, ,* David R. Clarke, Thermal Conductivity of the Gadolinium Calcium Silicate Apatites: Effect of Different Point Defect Types, *Acta Mater. 59 (2011) 3841–3850.*
6. J. Feng, B. Xiao, C. L.Wan, Z.X. Qu, Z.C. Huang, J.C. Chen, R. Zhou, *W Pan*, Electronic Structure, Mechanical properties and Thermal conductivity of $Ln_2Zr_2O_7$ (Ln = La, Pr, Nd, Sm, Eu and Gd) Pyrochlores, *Acta Mater. 59 (2011) 1742–176*
7. CL Wan, *W Pan,* Glasslike thermal conductivity in ytterbium doped lanthanum zirconate pyrochlore , *Acta Mater. 58 (2010) 6166–6172.*
8. CL Wan, *W Pan*, Influence of B site substituent Ti on structure and thermophysical properties of $A_2B_2O_7$-type pyrochlore $Gd_2Zr_2O_7$, *Acta Mater., 57 (2009) 4782–4789.*
9. J. Feng, B. Xiao, R. Zhou, *W. Pan*, Anisotropy in elasticity and thermal conductivity of monazite-type $REPO_4$ (RE = La, Ce, Nd, Sm, Eu and Gd) from first-principles calculations, *Acta Mater., 61 (2013) 7364–7383.*
10. XR Ren, *W Pan*, Mechanical properties of high temperature degraded yttria stabilized zirconia, *Acta Mater. 69 (2014) 397–406.*
11. Chen J, Lian J, Wang LM, Ewing RC, Wang RG, *Pan W*. X-ray photoelectron spectroscopy study of disordering in $Gd_2(Ti_{1-x}Zr_x)_2O_7$ pyrochlores. *Phys. Rev. Lett. 88(10), 105901 (2002).*

Publications on TBCs.

12. Wan CL, Qu ZX, He H, Luan D, *Pan W*, Ultralow thermal conductivity in highly anion-defective aluminates, *Phys. Rev. Lett. 101, 085901 (2008).*
13. J. Feng, C. Wan, B. Xiao, R. Zhou, *W Pan*, D. R. Clarke, Calculation of the thermal conductivity of $R_2SrAl_2O_7$ (R = La, Nd, Sm, Eu, Gd, Dy), *Phy. Rew. B, 84, 024302 (2011)*
14. Wan CL, *Pan W*, Xu Q, Qin YX, Wang JD, Qu ZX, Fang MH, Effect of point defects on the thermal transport properties of $(La_xGd_{1-x})_2Zr_2O_7$: Experiment and theoretical model. *Phys. Rev. B 74, 144109-1~9 (2006).*
15. J. Feng, B. Xiao, R. Zhou, and *W. Pan*, Eectronic and magnetic properties of double perovskite slab-rocksalt layer rare earth strontium aluminates natural superlattice structure, *J. Appl. Phys. 113, 143907 (2013)*
16. J. Feng, B. Xiao, R. Zhou, and *W. Pan*, Thermal expansions of $Ln_2Zr_2O_7$ (Ln=La, Nd, Sm, and Gd) pyrochlore, *J. Appl. Phys. 111, 103535 (2012).*
17. J. Feng, B. Xiao, Z. X. Qu, R. Zhou, and *W. Pan* , Mechanical properties of rare earth stannate pyrochlores *Appl. Phys. Lett., 99, 201909 (2011).*
18. *W Pan*, Simon R. Phillpot, Chunlei Wan, Aleksandr Chernatynskiy, Zhixue Qu, Low Thermal Conductivity Oxides, *MRS Bulleting. Vol 37 Oct 2012, 917-922.*
19. J. Feng, B. Xiao, R. Zhou and W. Pan, Thermal expansion and conductivity of $RE_2Sn_2O_7$ (RE = La, Nd, Sm, Gd, Er and Yb) pyrochlores, *Scripta Mater. 69 (2013) 401–404*
20. J Feng, B Xiao, R Zhou and *W Pan*, Thermal conductivity of rare earth zirconate pyrochlore from first principles, *Scripta Mater. 68 (2013) 727–730*
21. J Feng, XR Ren, XY Wang, R Zhou, *W Pan*, Thermal Conductivity of Ytterbia Stabilized Zirconia, *Scripta Mater.,66 (2012) pp. 41-44*
22. XR Ren, SC Guo, M Zhao, W Pan, Thermal conductivity and mechanical properties of $YSZ/LaPO_4$, *J. Mater Sci (2014) 49:2243–2251.*
23. Qu ZX, Wan CL, *Pan W*. Thermal expansion and defect chemistry of MgO-doped $Sm_2Zr_2O_7$. *Chem. Mater. 19 (20), 4913 (2007).*

Publications on TBCs.

24. Meng Zhao, Xiaorui Ren, and Wei Pan, Effect of Lattice Distortion and Disordering on the Mechanical Properties of Titania-Doped Yttria-Stabilized Zirconia, *J. Am. Ceram. Soc.,* 97 [5] 1566–1571 (2014)
25. CL Wan, ZX Qu, AB Du, *W Pan,* Order-disorder transition and unconventional thermal conductivities of the $(Sm_{1-x}Yb_x)_2Zr_2O_7$ series, *J. Am. Ceram. Soc., 94 [2] 592–596 (2011).*
26. AB Du, CL Wan, ZX Qu, RF Wu, *W Pan* , Effects of the texture on the thermal conductivity of the $LaPO_4$ monazite , *J. Am. Ceram. Soc., 93 [9] 2822–2827 (2010).*
27. CL Wan, Taylor D. Sparks, *W Pan*, and David R. Clarke, Thermal Conductivity of the Rare-Earth Strontium Aluminates, *J. Am. Ceram. Soc., 93 [5] 1457–1460 (2010)*
28. AB Du, CL Wan, ZX Qu, *W Pan*, Thermal transport properties of monazite-type $RePO_4$(Re = La, Ce, Nd, Sm, Eu, Gd), *J. Am. Ceram. Soc., 92 [11] 2687–2692 (2009).*
29. Xu Q, *Pan W*, Wang JD, Wan CL, Qi LH, Miao HZ, Mori K, Torigoe T, Rare- earth zirconate ceramics with fluorite structure for thermal barrier coatings. *J. Am. Ceram. Soc. 89 (1), 340 (2006).*
30. *Pan W*, Shi SL. Microstructure and mechanical properties of Ti_3SiC_2/3Y-TZP composites by spark plasma sintering. *J. Eur. Ceram. Soc. 27 (1), 413 (2007).*
31. *Pan W*, Wan CL, Xu Q, Wang JD, Qu ZX, Thermal diffusivity of samarium- gadolinium zirconate solid solutions. *Thermolchim. Acta 455 (1-2), 16 (2007).*
32. J. Feng, B. Xiao, C. Wan, Z. Qu, R. Zhou, *W Pan*, Electronic and elastic properties of a double perovskite slab–rocksalt layer of $Eu_2SrAl_2O_7$ investigated by LSDA + U, *Solid State Communications 151 (2011) 1326–1330*
33. Xu Q, *Pan W*, Wang JD, Qi LH, Miao HZ, Mori K, Torigoe T. Preparation and thermophysical properties of $Dy_2Zr_2O_7$ ceramic for thermal barrier coatings. *Mater. Lett. 59, 2804 (2005).*

清華大學 Tsinghua University

Thanks for your attention!